AD-A092 959 AIR FORCE WEAPONS LAB KIRTLAND AFB NM F/G 20/6
FIBER OPTIC TRANSMITTER AND RECEIVER RADIATION EVALUATION.(U)
SEP 80 B DEVE, K LOREE
UNCLASSIFIED AFWL-TR-79-168 NL

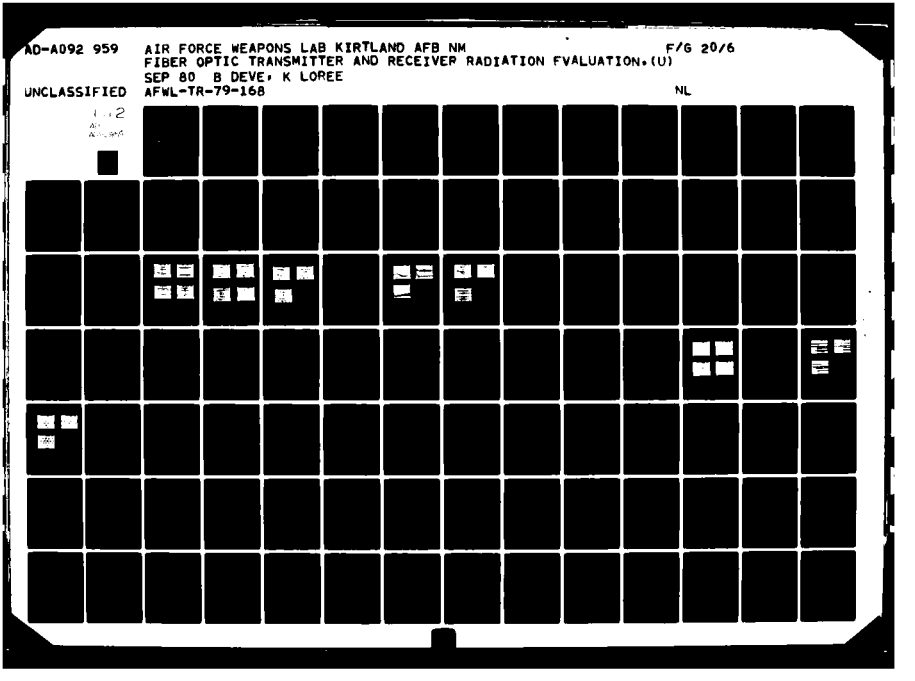

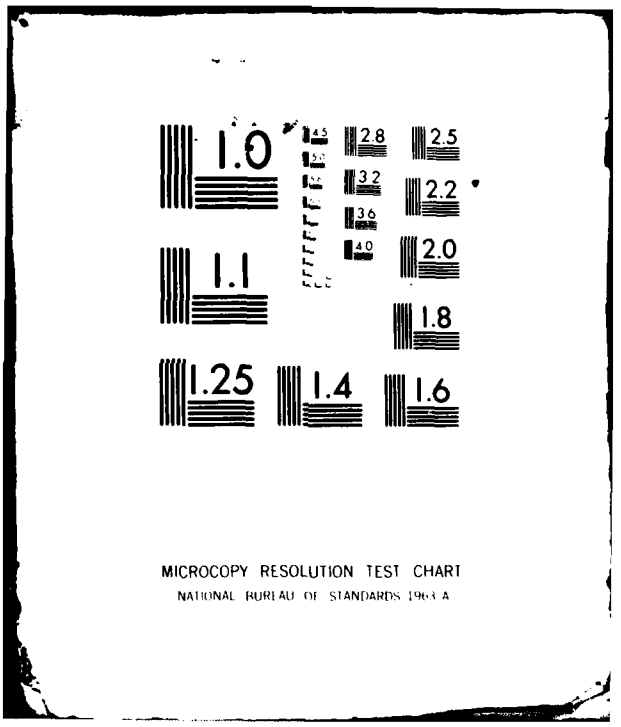
1.0
2.8
2.5
3.2
2.2
3.6
4.0
2.0
1.1
1.8
1.25
1.4
1.6
MICROCOPY RESOLUTION TEST CHART
NATIONAL BUREAU OF STANDARDS 1963 A

AFWL-TR-79-168

LEVEL II 12 SC

AFWL-TR-79-168

AD A092959

FIBER OPTIC TRANSMITTER AND RECEIVER RADIATION EVALUATION

Bernd Deve
Keith Loree

September 1980

Final Report

Approved for public release; distribution unlimited.

This research was sponsored by the Defense Nuclear Agency under Subtask: Z99QAXTB029, Radiation Effects on MSI/LSI; Work Unit 62, Radiation Characterization of MSI/LSI.

Prepared for
Director
DEFENSE NUCLEAR AGENCY
Washington, DC 20305

AIR FORCE WEAPONS LABORATORY
Air Force Systems Command
Kirtland Air Force Base, NM 87117

AFWL-TR-79-168

This final report was prepared by the Air Force Weapons Laboratory, Kirtland Air Force Base, New Mexico, under Job Order WDNE3101. Lieutenant Keith Loree (NTYCT) was the Laboratory Project Officer-in-Charge.

When US Government drawings, specifications, or other data are used for any purpose other than a definitely related Government procurement operation, the Government thereby incurs no responsibility nor any obligation whatsoever, and the fact that the Government may have formulated, furnished, or in any way supplied the said drawings, specifications, or other data, is not to be regarded by implication or otherwise, as in any manner licensing the holder or any other person or corporation, or conveying any rights or permission to manufacture, use, or sell any patented invention that may in any way be related thereto.

This report has been authored by an employee of the United States Government. Accordingly, the United States Government retains a nonexclusive, royalty-free license to publish or reproduce the material contained herein, or allow others to do so, for the United States Government purposes.

This report has been reviewed by the Public Affairs Office and is releasable to the National Technical Information Service (NTIS). At NTIS, it will be available to the general public, including foreign nations.

This technical report has been reviewed and is approved for publication.

KEITH LOREE
2d Lt, USAF
Project Officer

CHARLES A. AEBY
Chief, Satellite & C^3 Branch

FOR THE DIRECTOR

NORMAN K. BLOCKER
Colonel, USAF
Chief, Applied Physics Division

DO NOT RETURN THIS COPY. RETAIN OR DESTROY

UNCLASSIFIED

SECURITY CLASSIFICATION OF THIS PAGE (When Data Entered)

REPORT DOCUMENTATION PAGE

READ INSTRUCTIONS BEFORE COMPLETING FORM

1. REPORT NUMBER: AFWL-TR-79-168	2. GOVT ACCESSION NO.: AD-A092 959
3. RECIPIENT'S CATALOG NUMBER:	
4. TITLE (and Subtitle): FIBER OPTIC TRANSMITTER AND RECEIVER RADIATION EVALUATION	5. TYPE OF REPORT & PERIOD COVERED: Final Report
	6. PERFORMING ORG. REPORT NUMBER:
7. AUTHOR(s): Bernd Deve Keith Loree, 2Lt, USAF	8. CONTRACT OR GRANT NUMBER(s): WDNE, Z99QAXT
9. PERFORMING ORGANIZATION NAME AND ADDRESS: Air Force Weapons Laboratory (NTYCT) Kirtland Air Force Base, NM 87117	10. PROGRAM ELEMENT, PROJECT, TASK AREA & WORK UNIT NUMBERS: 62704H/WDNE3101 31 B029
11. CONTROLLING OFFICE NAME AND ADDRESS: Air Force Weapons Laboratory (NTES) Kirtland Air Force Base, NM 87117	12. REPORT DATE: September 1980 13. NUMBER OF PAGES: 98 97
14. MONITORING AGENCY NAME & ADDRESS (if different from Controlling Office): Director Defense Nuclear Agency Washington, D.C. 20305	15. SECURITY CLASS. (of this report): UNCLASSIFIED 15a. DECLASSIFICATION/DOWNGRADING SCHEDULE

16. DISTRIBUTION STATEMENT (of this Report)

Approved for public release; distribution unlimited.

17. DISTRIBUTION STATEMENT (of the abstract entered in Block 20, if different from Report)

18. SUPPLEMENTARY NOTES

This research was sponsored by the Defense Nuclear Agency under Subtask: Z99QAXTB029, Radiation Effects on MSI/LSI; Work Unit 62, Radiation Characterization of MSI/LSI.

19. KEY WORDS (Continue on reverse side if necessary and identify by block number)

Fiber Optics	TTL	Ionizing Dose Rate
Transmitter	Neutron Radiation	Radiation Response
Receiver	Gamma Radiation	Failure Analysis
Integrated Circuit		
Module		

20. ABSTRACT (Continue on reverse side if necessary and identify by block number)

The report describes the radiation characterization of fiber optic transmitter and receiver integrated circuits developed by the Air Force Avionics Laboratory. These devices were manufactured by Spectronics of Honeywell and the model numbers are SPX 3619, SPX 3620, SPX 4125 and SPX 4126. Nuclear radiation hardness was not a specific goal in the development of these integrated circuits. The devices were evaluated for catastrophic failure and performance degradation in a neutron and total gamma dose environments. Possible latch-up and transient upset were evaluated in an ionizing dose rate environment.

DD FORM 1 JAN 73 1473

UNCLASSIFIED

SECURITY CLASSIFICATION OF THIS PAGE (When Data Entered)

013150

JOB

CONTENTS

INTRODUCTION

This report describes the radiation testing performed on fiber optic transmitter and receiver integrated circuits (IC) developed for the Air Force Avionics Laboratory (AFAL) under a Honeywell contract. The objective of the program was to develop low cost fiber optic modules for transmission and reception of digital data via fiber optic bundles (data rates of 10 kbits/s to 10 Mbits/s). The integrated circuits were optimized for producibility, wide usage, low cost, high reliability and electromagnetic interference/ electromagnetic pulse (EMI/EMP). Nuclear radiation hardness was not a goal of this development program. Two AFAL technical reports describe in detail the design, fabrication, and testing of the receivers and transmitters used for radiation testing (Refs. 1 and 2). In order to realize the full potential of these low cost ICs in operational and upcoming systems, future acquisition costs must also be low. The ICs are now commercially available and produced by Spectronics (Receiver SPX 3620; Transmitter SPX 3619).

Following delivery of parts from Honeywell, AFAL provided AFWL with 30 receivers and 30 transmitters for radiation evaluation. The radiation testing was partially funded by AFAL, as AFAL covered the cost of radiation facility use. The radiation tests were performed between May 1979 and October 1979.

In addition to the radiation test results, the electrical and radiation test procedures are also discussed in this report. Due to difficulties experienced in receiver operation as initially described in AFWL's test plan previously submitted to AFAL, Section II of this report covers the updated test circuitry and measurement procedures. Section III covers the radiation test results. The intent of this work was to determine the device failure

---

1. Elmer, Ben R., Fiber Optics Receiver Integrated Circuit Development, AFAL-TR-78-185, Air Force Avionics Laboratory, Wright-Patterson Air Force Base, Ohio, December 1978.

2. Elmer, Ben R., Fiber Optics Transmitter Integrated Circuit Development, AFAL-TR-78-107, Air Force Avionics Laboratory, Wright-Patterson Air Force Base, Ohio, July 1978.

levels in various radiation environments, not to perform a detailed analysis of failure mechanisms. Radiation tests were conducted in total gamma dose (Co-60), neutron, and ionizing dose-rate (Flash X-ray) environments. The transmitter and receiver operated well after neutron and total dose environments, but the receiver was at best marginal after transient radiation tests.

Sections V-VII of this report describe the radiation characterization tests that were performed on fiber optic transmitter and receiver modules (SPX 4125 and SPX 4126, respectively) manufactured by Spectronics of Honeywell under contract to the AFAL. The modules are self-contained packages that incorporate the ICs tested in Sections II-IV of this report and Spectronics optical diodes. The testing and evaluation was performed during the period between December 1979 and March 1980.

The electrical and radiation test procedures are described, and the radiation test results are discussed. The modular construction of these devices prevented the use of many measurement methods used in Sections II-IV. Therefore, no direct comparison of test data can be made.

II. ELECTRICAL TESTING (SPX 3619, SPX 3620)

The following is a description of the electrical testing procedures used for preirradiation and subsequent incremental irradiation evaluations. However, before discussing the transmitter and receiver tests, circuit designs used to perform the testing are presented.

SYSTEM CONFIGURATION

The initial fiber optic system configuration is given in Figure 1a. Several changes were made in the physical layout of the fiber optic transmitter and receiver system. The light-emitting diode (LED) and photodiode detector were located 0.5 m from the transmitter and receiver printed circuit boards for easier shielding in radiation environments. No problems appeared to arise from this arrangement and hardly any bit errors resulted (bit error rate (BER) of 10^{-10} to 10^{-11} error/s. However, it was later discovered that the photodiode current (I_I) was approximately 40 μA instead of the desired operating range of 250-500 nA. This large current resulted in the very few bit errors observed. Lowering the photodiode current to 500 nA caused oscillations in the fiber optic output. The fiber optic system was then redesigned (Figure 1b) to allow closer placement of the photodiode to the sensitive receiver integrated circuit (FORIC). However, due to frequent interchange of receivers during testing, it was imperative to use an IC socket for easier part removal and insertion. The socket capacitance still caused problems in the fiber optic operation at low photodiode current levels. To obtain the desired current levels (< 500 nA), the receiver photodiode input pin (pin 5) was bent up and soldered directly to the photodiode anode. The total length from the pin lead of the receiver to the photodiode case was 1 cm. Typical minimal operating currents observed in the receivers were 200-300 nA, depending upon the individual receiver. To be more confident of proper fiber optic system and error detection circuit operation, a bit error introduction circuit was also added to the fiber optic transmitter (FOTIC) board. When activated, the circuit would eliminate a positive pulse in the data stream to the transmitter. The error detection circuit would then catch the missing pulse and update the number of errors displayed by LEDs. Figures 2 and 3 give the component connections and values for the transmitter and the receiver.

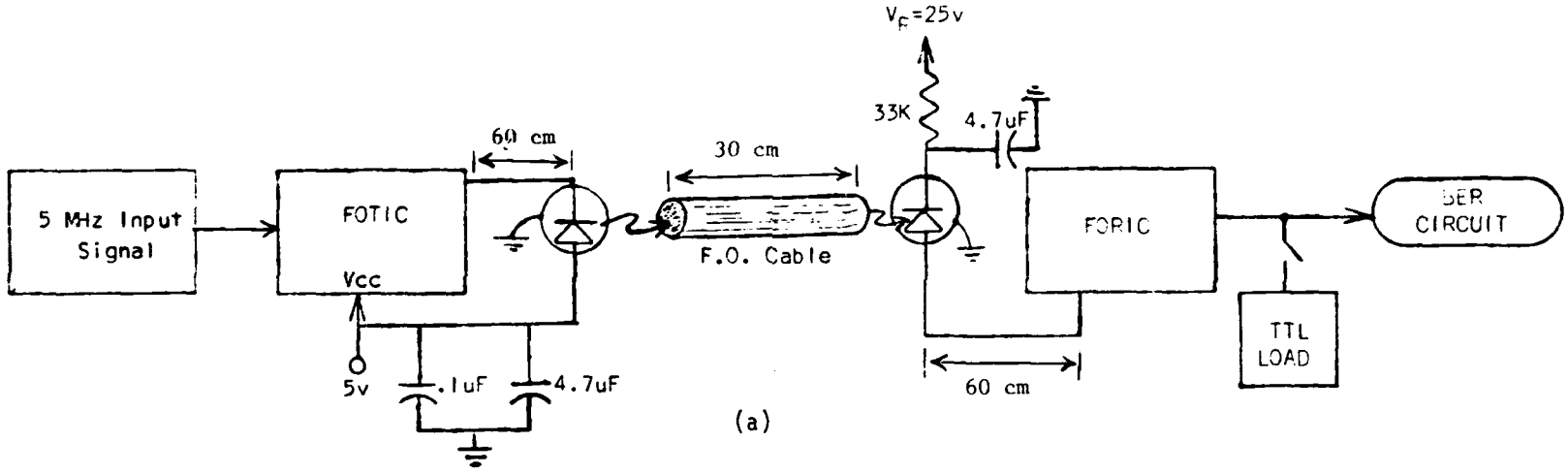

System Components:

Transmitter IC (FOTIC) - Spectronics 2144-2
Reciever IC (FORIC) - Spectronics 2145-2
Optic transmitter - Spectronics SE 2231 LED
Optic reciever - Spectronics SD 3478 photodiode
Optic cable - CROFON cable

Figure 1a. Initial fiber optic test system configuration

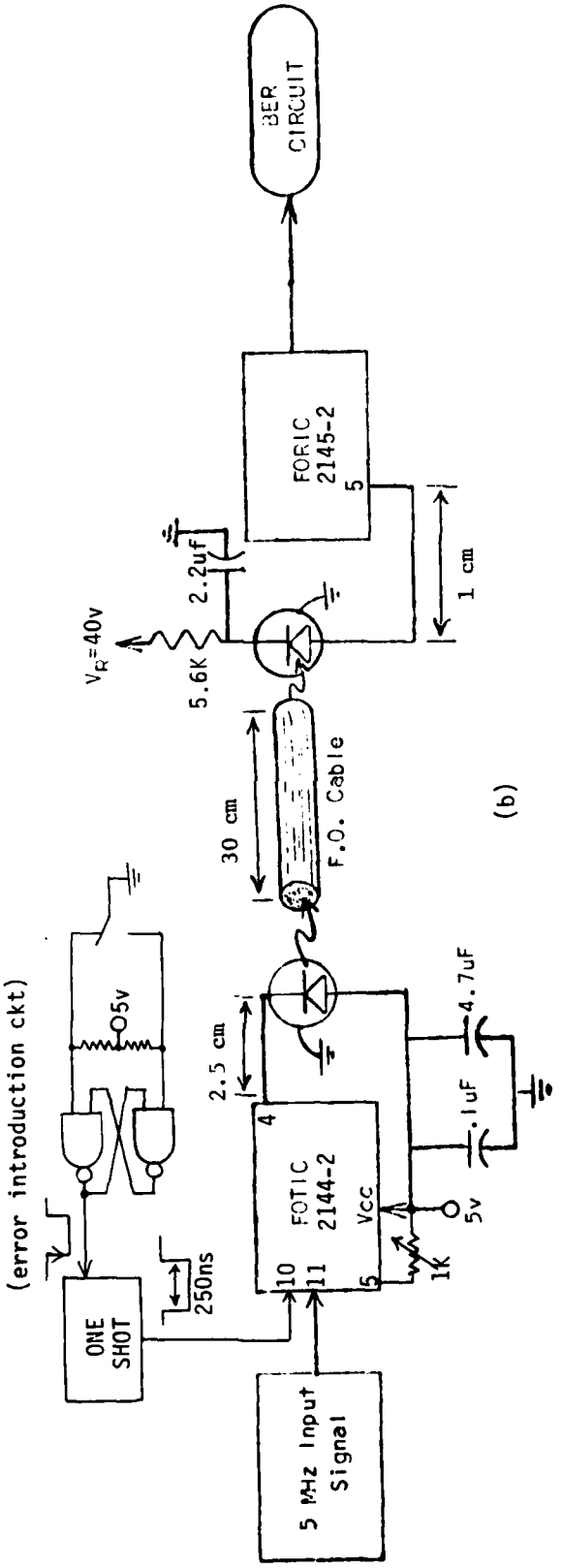

Figure 1b. Current configuration with error introduction and short photodiode lead lengths

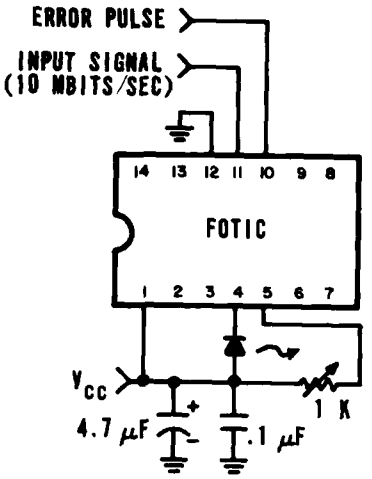

Figure 2. Transmitter component values and connections

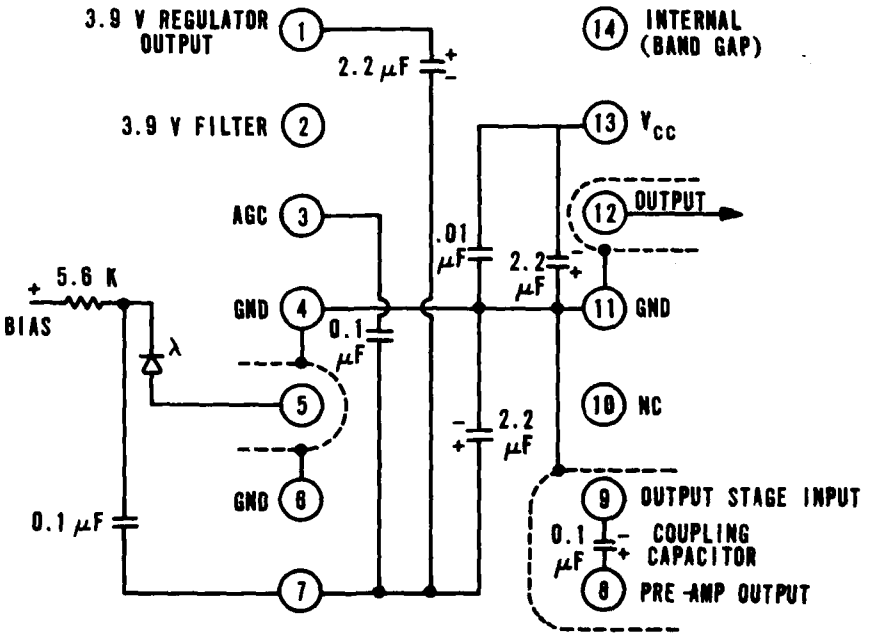

Figure 3. Receiver internal components and connections

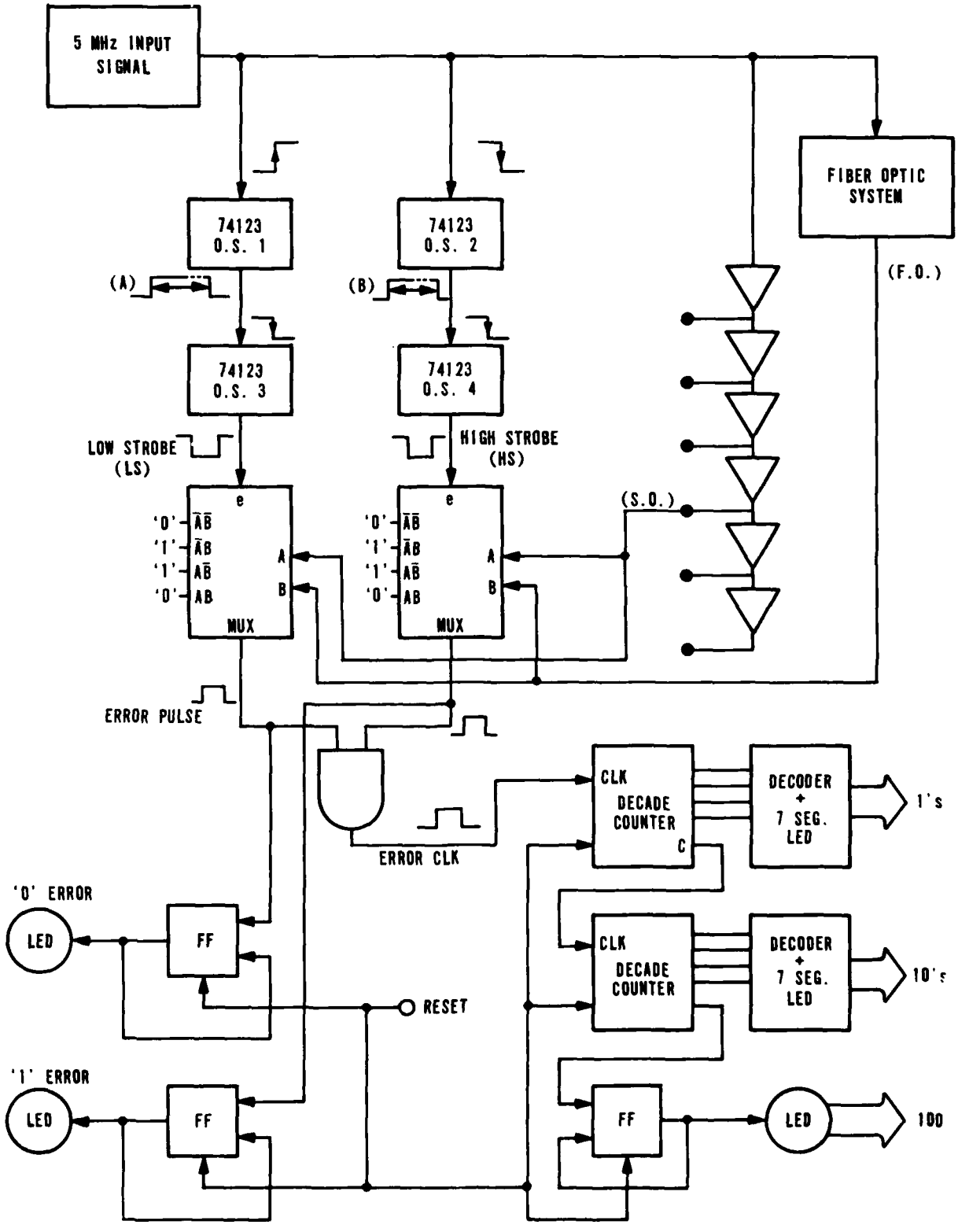

Figure 4a. Error detector circuit and timing diagram

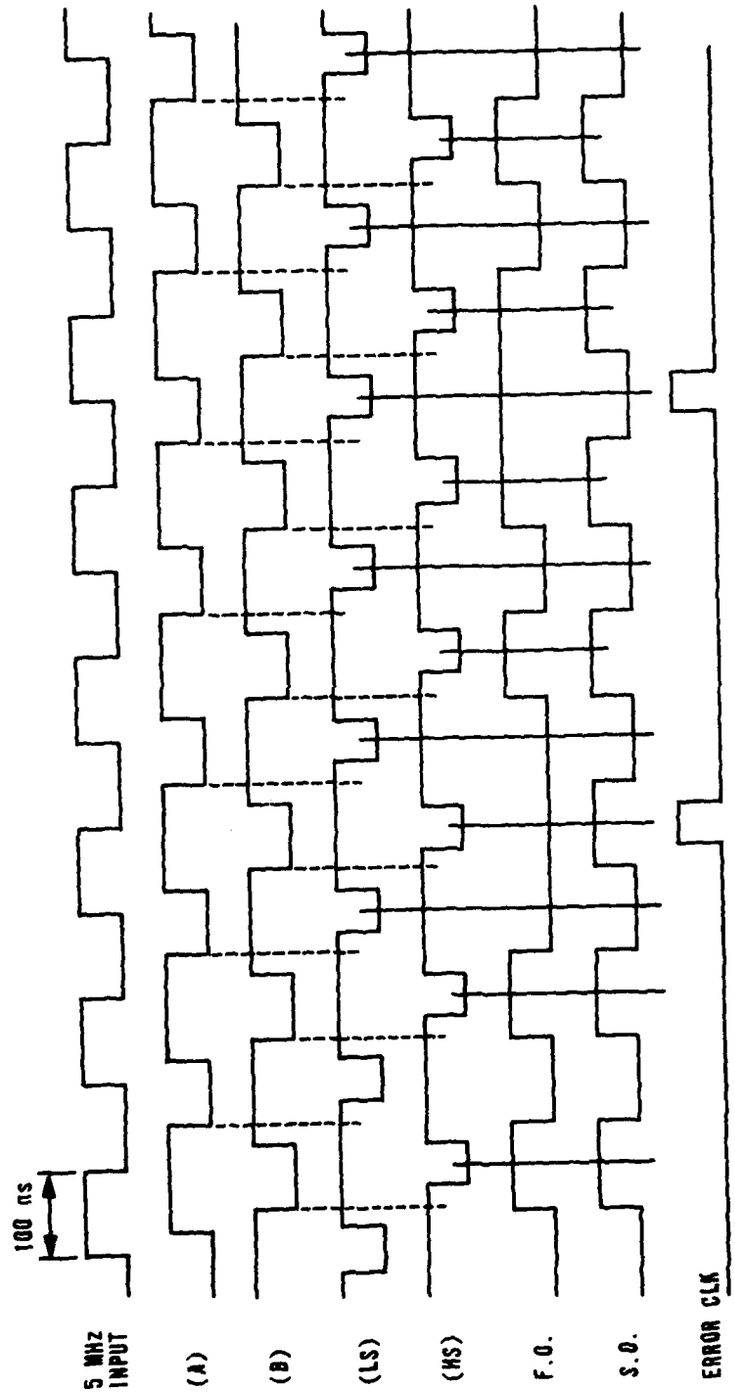

Figure 4b. Timing diagram

Figure 4 shows a block diagram of the error detecting circuit and a timing diagram. The following is a brief description of the operation of the error detection circuit. A 5 MHz (50% duty cycle) signal is applied simultaneously to the fiber optic system and to the error detection circuit. Propagation delay time of the input signal through the fiber optic system is 40-70 ns using a short fiber link of 15 cm. To simulate this output for error detecting purposes, the input signal is delayed through hex buffers. The delayed output most closely matching the fiber optic output (F.O.) is used as the simulated output (S.O.). Strobe signals are also needed to compare the F.O. and S.O. signals during the ZERO and ONE state. Multivibrators 3 and 4 (O.S.3 and O.S.4) are fixed for a 45 ns negative outgoing output pulses and are used as the strobes to enable the multiplexers which do the actual comparison. Multivibrators 1 and 2 are variable output pulse lengths used to position the strobes with respect to the simulated output. Multivibrator 3 is used as a strobe that enables MUX 2 when the simulated output is low. Likewise, multivibrator 4 strobes MUX 1 when the simulated output is high. The MUX outputs are ANDED together and a 45 ns pulse results whenever an error occurs (when F.O. and S.O. do not match during the MUX enable pulses). Any resulting errors are then counted by decade counter ICs, decoded for 7-segment digits, and then displayed on LEDs. If over 100 errors result, a flip-top is set which drives an LED signifying that over 100 errors occurred. The fiber optic output, simulated output, and strobes are always monitored on a dual beam oscilloscope.

TRANSMITTER TESTS

Transmitter tests involve verification of operation and measurement of input (pins 10 and 11) and output currents in both the ZERO and ONE states. Rather than performing the current measurements manually, a short routine was set up on an ALMA 480 bench-top integrated circuit tester.

Ten measurements are made using the IC tester. The first four are LED "on" current measurements with pin 7 grounded, then pin 8 grounded, then pin 9 grounded, and finally pins 7, 8 and 9 grounded. There is no LED used with the FOTIC in these tests. Instead of an LED, pin 4 is connected to a 2.5 V bias with the current monitored by the tester. Test 5 measures the LED "off" current at pin 4 with an input set to a ZERO state. Test 6 measures the IC power supply current draw (Icc). The last four tests measure the

ZERO and ONE state input currents, at the input (pins 10 and 11). Table 1 shows a sample data sheet filled with typical values.

TABLE 1. SAMPLE ALMA 480 TRANSMITTER DATA SHEET

TRANSMITTER No. 18	DATE: LEVEL:	5/30 Pre RAD	6/1 $5x10^{12}$	6/6 $1x10^{13}$	6/8 $4x10^{13}$	6/12 $7x10^{13}$	6/13 $1x10^{14}$	6/14 $4x10^{14}$	6/27 $7x10^{14}$
		Input:		Measure:	Typical Data:				
		Pin 10	Pin 11						
I_d - 50mA	(mA)	'1'	'1'	Pin 4	50 mA				
I_d - 75mA	(mA)	'1'	'1'	Pin 4	75 mA				
I_d - 25mA	(mA)	'1'	'1'	Pin 4	25 mA				
I_d - 150mA	(mA)	'1'	'1'	Pin 4	150 mA				
I_d - off	(uA)	'0'	'1'	Pin 4	2 uA				
I_{cc}	(mA)	'0'	'1'	Pin 1	30 mA				
I_{IL} - PIN 10	(mA)	'0'	'1'	Pin 10	-1.1 mA				
I_{IH} - PIN 11	(uA)	'0'	'1'	Pin 11	0.05 uA				
I_{IL} - PIN 11	(mA)	'1'	'0'	Pin 11	-1.1 mA				
I_{IH} - PIN 10	(uA)	'1'	'0'	Pin 10	0.05 uA				

SAMPLE DATA SHEET SHOWING TYPICAL CURRENT VALUES

V_{cc} = 5.5 volts
'1' input = 2.4 volts
'0' input = 0.4 volts

Before the above tests were performed, the transmitters were all checked for proper operation in the fiber optic system using the error detection circuit. Following verification of operation, a test is performed on the transmitter to determine the radiation degradation of drive current at low current levels which are not tested by the ALMA 480. The test consists of setting up the control receiver (FORIC-1) and control transmitter (FOTIC-1) in the fiber optic system for 250 nA photodiode current. FOTIC-1 is then removed without changing the LED current level. Attenuation of the fiber optic signal seen at the photodiode receiver is controlled by reducing the LED drive current with a variable resistor tied to the transmitter's output transistor emitter. Thus degradation of the irradiated transmitter's drive capability as compared to that of FOTIC-1 will result in a lower photodiode current. The irradiated transmitters are placed in the circuit and the corresponding photodiode current is measured. This test allows comparison

of the irradiated transmitter current to that of the control device and to preirradiation current levels. To prevent any reduction of damage by high current annealing (especially after Co-60 irradiation), the transmitter tests in the fiber optic system, which use approximately 1 mA LED current (Id), are performed before the ALMA 480 tests which involve 150 mA current tests.

RECEIVER TESTS

All tests on the fiber optic receiver (FORIC) were performed in the fiber optic system in conjunction with the error detection circuit. The ALMA 480 cannot measure very low input current, and it also has a limited bandwidth of 10 kHz which renders it useless for any realistic receiver testing.

All bit error rate (BER) measurements including postradiation tests were performed with a data stream of 10 Mbits/s (5 MHz square wave). The 5 MHz square wave is identical to 10 Mbit/s Manchester coded alternating ZERO/ONE pattern as seen in Figure 5. At a photodiode current of 250 nA and input signal of 5 Mbits/s, the FORIC BER should be less than 10^{-8} bit errors/s. To have some confidence in the BER measurement, the test was run at 5 Mbits/s for 16½ minutes to obtain 10^{10} pulses per test. Due to the length of time required to test each receiver, the BER measurements were not made under various output loading conditions. The FORIC output load was one TTL load (the output is used as an input to the multiplexer in the error detecting circuit).

As mentioned earlier, all the receivers had pin 5 (photodiode input) turned up and soldered directly to the photodiode so that the desired operating range of 250-500 nA could be achieved while having the device in a low insertion force socket for easy testing. The BER is very dependent upon the photodiode current (I_I) level as seen below in a measurement made on FOTIC-1 and FORIC-1 pair at 5 Mbits/s.

CURRENT (I_I)	BIT ERRORS	BIT ERROR RATE
250 nA	100/2 s	5.0×10^{-6}
210 nA	170/30 s	5.6×10^{-7}
215 nA	52/30 s	1.7×10^{-7}
220 nA	14/10 min	2.3×10^{-9}
225 nA	16/1 h	4.4×10^{-10}
230 nA	6/2 h	8.3×10^{-11}

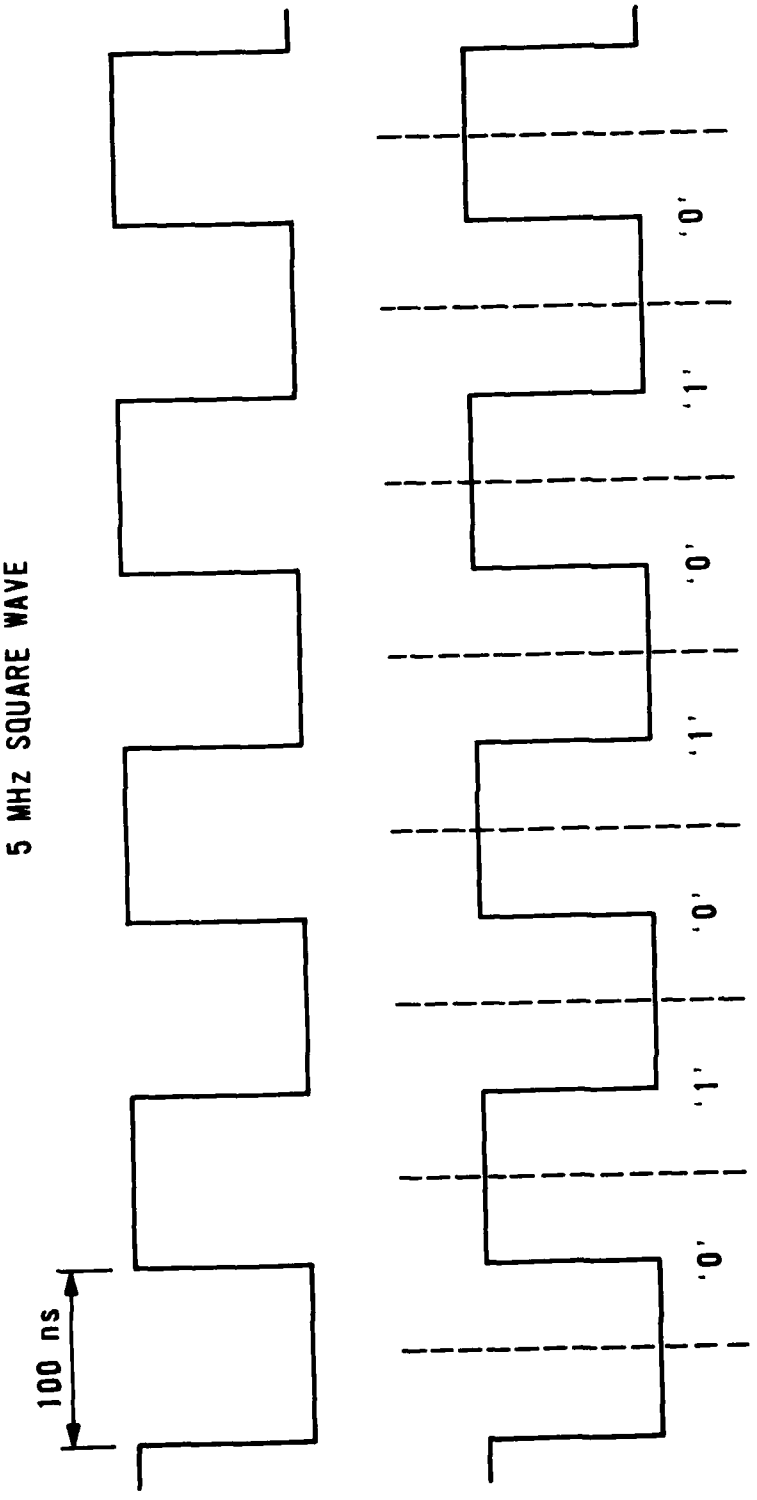

Figure 5. Manchester coded data (5 Mbits/s).

For this receiver, a photodiode current below 200 nA causes severe oscillations at the receiver output. Thus, an effective way to observe radiation damage is to note any variation in the minimum current of operation for a given receiver. Depending upon the solder connection at pin 5, the seating of the device in the socket, and drift of the nanoampere current meter, it was not uncommon to observe 30-40 nA differences in minimum current on repetitive insertions of the same receiver. The BER test was performed 20 nA above the minimal operational current. Minimal operational current was chosen to be a point where the oscilloscope showed a clean output waveform and the LED error counter would not register any errors in approximately a 5-15 s time span. Thus in the photodiode current versus BER data just presented, the minimum current for FORIC-1 would be about 220 nA and the BER test would be performed at 240 nA. Photodiode current measurements were made with a HP435 micro volt-ampere meter. Photodiode off current measured with the FOTIC input set to ZERO, consistently read 5-6 nA (both pre- and post-irradiation) for all receivers. The meter displays the DC average input of both the ZERO and ONE state. For example, a meter reading of 110 nA (50% duty cycle input) indicates a photodiode ONE current of 215 nA and ZERO current of 5 nA. For data taken during the tests, a meter reading of 110 nA was just doubled to 220 nA and recorded as such. Thus the minium current is actually slightly lower (5 nA) than indicated in the data.

III. RADIATION TEST RESULTS (SPX 3619, SPX 3620)

The following approach was used to perform the BER measurements on test devices. One transmitter designated (FOTIC-1) was used only to test all receivers before and after irradiation. FOTIC-1 was used as a control device and never irradiated. Similarly, one receiver (FORIC-1) was used to test all the transmitters before and after radiation in the fiber optic system. Methods of BER receiver tests and transmitter tests were described in Section II. Line voltage transients (caused by turning electrical equipment on or off) occasionally resulted in additional bit error count. Even including these sporadic error as actual fiber optic bit errors, the BER is still better than 10^{-8} bit errors/s for every device both pre- and postirradiation.

TOTAL DOSE TESTS

Seven transmitters and nine receivers were tested in a Co-60 radiation environment. The number of transmitters tested was reduced to seven, since four devices were ruined during initial programming of the ALMA 480 tests. Device evaluations were performed after 1, 5, 10, 50 and 100 krads, 1 Mrad, 5 Mrads(Si). AFWL's 5-kCi Co-60 facility was used for tests up to and including 1 Mrad total dose. The 5 Mrad test was made nearly 3 weeks later at Sandia Laboratory's 80 kCi Co-60 Gamma Irradiation Facility (GIF). To prevent any room temperature annealing following irradiation and prior to testing a device, the integrated circuits were suspended above liquid nitrogen to keep them cool. The bias configurations for the receivers and transmitters tested are given in Table 2.

TABLE 2. BIAS CONFIGURATIONS FOR RECEIVERS/TRANSMITTERS

TRANSMITTERS		RECEIVERS	
Dev. No.	Bias	Dev. No.	Bias
5	Unbiased	1	Unbiased
6	Unbiased	9	Unbiased
4	Biased/Input GND	17	Unbiased
7	Biased/Input FND	3	Biased/Input GND
3	Biased/Input + 5 V	29	Biased/Input GND
9	Biased/Input + 5 V	5	Biased/Input + 5 V
8	Biased/Input CLK	30	Biased/Input CLK
		8	Biased/Input CLK

Table 3 gives the minimum operating current for the receiver.

TABLE 3. MINIMUM OPERATING CURRENT (nA) VERSUS TOTAL DOSE (rads(Si))

DEV NO.	PRE	1	5	10	50	100	500	1M	PRE[a] 5M	5M
29	220	220	230	250	225	220	240	240	210	195
30	220	240	230	250	235	230	210	225	260	195
11	330	340	340	325	300	325	330	285	290	240
17	275	290	290	290	270	300	270	255	255	200
5	260	290	300	290	310	315	290	245	PIN	BROKE
3	220	230	250	260	240	240	250	230	230	205
8	225	240	230	230	200	230	230	215	230	190
9	220	240	230	230	220	240	220	230	200	170
1	285	290	250	260	240	260	250	240	210	170

[a](Pre 5 Mrad test measurements were made because 20 days had elapsed since the 1 Mrad tests were performed).

The minimum currents ranged from 170 nA to 340 nA for different receiver's photodiode current (I_I). Since, as stated earlier, the minimum operating current fluctuated by as much as 30-40 nA upon removal/reinsertion of the same device; the only significant radiation induced change observable in minimum current appeared after the 5 Mrad irradiation. There was a noticeable decrease in current levels indicating that the receiver sensitivity improved to where the average minimum current is now less than 200 nA. Receiver 5 had pin 5 fall off after 1 Mrad due to excessive bending.

TABLE 4. BIT ERROR RATE (x 10^{-10} bit errors/s) VERSUS TOTAL DOSE (rads (Si))

DEV NO.	PRE	1	5	10	50	100	500	1M	PRE 5M	5M
29	1	0	1	0	2	0	2	0	1	1
30	0	6	10	0	0	0	1	0	0	4
11	0	1	16	8	10	0	0	1	2	5
17	1	1	0	0	0	0	0	4	0	3
5	1	0	0	12	0	0	0	0	PIN	BROKE
3	0	0	0	0	0	0	0	19	3	10
8	0	0	0	0	1	7	0	0	0	0
9	0	3	1	0	0	0	0	1	0	0
1	0	0	0	0	0	0	1	0	0	0

0 - Less than 1 x 10^{-10} bit errors/s

As seen in Table 4, all BER measurements are well below the given specification of 10^{-8} bit errors/s. If no errors were observed after 15 minutes, the error rate is less than 1×10^{-10} bit errors/s and written in the table as a "0."

The transmitter data are given in Tables 5 through 7. Table 5 is an average of the data taken with the ALMA 480 IC tester. The LED drive current (Id), power supply current, LED off current, and input current all decreased with total dose exposure. The typical LED current decrease was less than 5 percent after 5 Mrad(Si), Table 5 does not include device 7 as part of the average (see Table 6), since a problem in the LED drive current and power supply current tests occurred somewhere between the 1 and 5 krad tests. The cause does not appear to be linked to total dose irradiaiton, since beyond 5 krads the device responds very uniformly. It is most unlikely that the device was inserted backwards in the socket or was electrically overstressed. One other interesting point about device 7 was that the LED off current always was an order of magnitude larger than the rest of the devices (20 μA versus 2 μA).

The individual ALMA 480 transmitter data sheets are given in the appendix. Table 7 shows the variation in transmitter current (while operating in the fiber optic system) as measured by the receiver photodiode current. The table has no data until after 50 krads since this is when the test was originated. FORIC-1 and FOTIC-1 are set up for 250 nA photodiode current by adjusting the transmitter emitter resistance. The irradiated transmitters than replace FOTIC-1 in the circuit. Although no significant variation in transmitter current versus dose is seen, it also shows a problem with device 7. For the given transmitter emitter resistance, device 7 produces substantially less LED current as seen by the lower photodiode current than the remaining devices.

NEUTRON TESTS

Passive neutron irradiations were performed on the devices at Sandia's pulsed reactor (SPR II and SPR III). Table 8 shows the desired fluences and total fluence received by the 10 transmitters and 10 receivers as measured by sulfur dosimeters.

TRANSMITTER No. *AVG*	DATE: LEVEL:	5/17/79 PRE RAD	5/21/79 1.E+03	5/22/79 5.E+03	5/22/79 1.E+04	5/23/79 5.E+04	5/23/79 1.E+05	5/24/79 5.E+05	5/25/79 1.E+06	6/14/79 5.E+06
I_d - 50mA	(mA)	50.917	50.783	50.683	50.650	50.483	50.233	50.083	50.067	48.700
I_d - 75mA	(mA)	75.517	75.433	75.417	75.367	75.017	74.583	74.367	74.367	73.783
I_d - 25mA	(mA)	25.750	25.833	25.750	25.783	25.650	25.400	25.350	25.300	25.167
I_d - 150mA	(mA)	149.783	148.833	148.850	148.800	148.117	147.400	146.500	146.150	145.000
I_d - off	(uA)	1.970	1.920	1.979	1.882	1.863	1.842	1.822	1.796	1.639
I_{cc}	(mA)	32.000	31.983	31.967	31.967	31.850	31.683	31.517	31.433	31.150
I_{IL} - PIN 10	(mA)	-1.103	-1.119	-1.118	-1.116	-1.114	-1.108	-1.098	-1.087	-1.067
I_{IH} - PIN 11	(uA)	.029	.045	.093	.030	.027	.022	.041	.040	.016
I_{IL} - PIN 11	(mA)	-1.102	-1.118	-1.117	-1.115	-1.112	-1.106	-1.095	-1.085	-1.063
I_{IH} - PIN 10	(uA)	.026	.044	.088	.027	.025	.021	.037	.037	.015

TABLE 5. AVERAGE OF ALMA 480 CURRENT TESTS FOR SIX CO-60 IRRADIATED TRANSMITTERS.

TRANSMITTER No. 7	DATE:	5/17/79	5/21/79	5/22/79	5/22/79	5/23/79	5/23/79	5/24/79	5/25/79	6/14/79
	LEVEL:	PRE RAD	1.E+03	5.E+03	1.E+04	5.E+04	1.E+05	5.E+05	1.E+06	5.E+06
I_d - 50mA	(mA)	50.500	50.200	40.600	40.900	40.800	40.600	40.600	40.400	40.500
I_d - 75mA	(mA)	74.900	74.600	59.800	60.100	60.000	59.700	59.600	59.400	59.300
I_d - 25mA	(mA)	25.300	25.400	20.700	20.900	20.800	20.700	20.700	20.600	20.700
I_d - 150mA	(mA)	148.400	146.500	115.400	116.000	115.700	115.100	114.500	114.300	112.600
I_d - off	(uA)	19.500	19.100	18.220	17.900	18.140	18.230	18.460	18.410	18.580
I_{cc}	(mA)	31.300	18.100	18.200	18.200	18.300	18.300	18.400	18.400	18.400
I_{IL} - PIN 10	(mA)	-1.109	-1.126	-1.125	-1.128	-1.124	-1.120	-1.105	-1.100	-1.077
I_{IH} - PIN 11	(uA)	.030	.031	.092	.023	.022	.017	.032	.037	.014
I_{IL} - PIN 11	(mA)	-1.109	-1.126	-1.125	-1.127	-1.123	-1.116	-1.105	-1.098	-1.076
I_{IH} - PIN 10	(uA)	.027	.027	.082	.020	.020	.017	.029	.035	.013

TABLE 6. ALMA 480 CURRENT TESTS FOR TRANSMITTER NO. 7

TABLE 7. TRANSMITTER CURRENT VARIATION AS MEASURED BY RECEIVER PHOTOCURRENT (nA)

DEV	PRE	1	5	10	50	100	500	1M	5M
3	-	-	-	-	265	265	270	265	270
4	-	-	-	-	270	265	265	265	265
5	-	-	-	-	265	260	265	265	260
6	-	-	-	-	260	265	265	265	260
7	-	-	-	-	185	180	180	180	180
8	-	-	-	-	280	280	280	280	285
9	-	-	-	-	290	280	285	285	285

TABLE 8. FLUENCES FOR RECEIVERS/TRANSMITTERS.

DESIRED FLUENCE (n/cm^2)	FLUENCE RECEIVED (1 MeV equiv.) (n/cm^2)
5×10^{12}	4.1×10^{12}
1×10^{13}	1.0×10^{13}
4×10^{13}	3.3×10^{13}
7×10^{13}	7.3×10^{13}
1×10^{14}	1.3×10^{14}
4×10^{14}	3.9×10^{14}
7×10^{14}	7.5×10^{14}

On two occasions SPR facility operators unbent pin 5 of the receivers. Bending the pin back up for testing caused leads to break off on several receivers. The replacement of these broken devices with new ones cause the receiver minimum current (Table 9) and BER tables to appear a bit disorganized.

TABLE 9. MINIMUM RECEIVER PHOTODIODE CURRENT (nA) VERSUS FLUENCE (n/cm^2)

DEVICE NO.	PRE	$5x10^{12}$	10^{13}	$4x10^{13}$	$7x10^{13}$	10^{14}	4×10^{14}	$7x10^{14}$
2	260	270	260	(PIN BROKE		-	-	-)
4	245	(PIN BROKE		-	-	-	-	-)
6	245	240	240	250	230	220	190	2000
7	265	265	260	250	255	255	190	1500
10	250	240	240	245	235	230	170	1500
12	260	260	260	(PIN BROKE		-	-	-)
13	270	270	255	265	250	245	180	1500
15	245	250	240	245	245	235	175	2000
16	270	280	275	290	290	280	155	1500
18	240	230	240	220	235	215	155	1000
25	210	N	210	200	200	205	480	5000
23	295	N	N	N	260	290	220	2000
24	270	N	N	N	260	270	200	2000
26	260	N	N	N	310	310	150	4000

N - Not tested or irradiated at given level

The receivers had photodiode currents in the 250 nA range until 4×10^{14} n/cm^2 when a dramatic decline in minimal operating current resulted in 10 of 11 devices. The other device (receiver no. 25) was already experiencing the beginning of a sharp increase in minimum current that every device exhibited at 7×10^{14} n/cm^2. At 7×10^{14} there was no output pulse, just a steady state response until the current was increased to the value given in the table. Table 10 gives the BER for the receivers in the neutron environment.

The BER for the neutron irradiated devices was also less than the specification of 1×10^{-8} bit errors/s, although the photodiode current at 7×10^{14} n/cm^2 was an order of magnitude above that set for specification of the BER. It should also be restated that the given BER rates include any errors induced by line voltage transients and that the actual BER rates are, therefore, somewhat better than those given in the tables.

TABLE 10. BIT ERROR RATE (x 10^{10} bit errors/s)

DEVICE NO.	PRE	$5x10^{12}$	10^{13}	$4x10^{13}$	$7x10^{13}$	10^{14}	$4x10^{14}$	$7x10^{14}$
2	2	6	8	(PIN BROKE		-	-	-)
4	0	(PIN BROKE		-	-	-	-	-)
6	2	1	1	0	3	0	0	-
7	2	0	0	1	1	1	0	0
10	0	0	1	0	1	0	0	0
12	0	13	7	(PIN BROKE		-	-	-)
13	0	4	3	14	1	1	7	0
15	0	4	0	4	1	2	4	2
16	6	0	0	0	0	0	1	0
18	1	0	0	0	4	0	1	2
25	11	11	0	1	4	0	3	0
23	0	N	N	N	18	22	0	0
24	2	N	N	N	11	1	1	0
26	1	N	N	N	6	3	2	0

0 - Less than 1 x 10^{10} bit errors/s (0 errors in 15 min)

N - Not tested

Table 11 is an average of the ALMA 480 tests on the 10 transmitters at the various fluence levels. The main effects of neutron damage on the fiber optic transmitter are decreases in LED drive current, LED off current, and power supply current. LED drive current decreased by 5 percent of preirradiation levels after 4 x 10^{14} and by 12 percent after 7 x 10^{14} n/cm^2. The table also hows a large difference in high input current levels (I_{IH}) between transmitter input pins 10 and 11 (ALMA tests 8 and 10). This was caused by transmitter 17 which had an input high current at pin 10 of 3.3 μA instead of a typical device's current of 0.03 μA. The individual ALMA 480 data sheets are given in the appendix. Table 12 gives the variation in transmitter current while operating in the fiber optic system as measured by the photodiode current (FORIC-1 and FOTIC-1 are set up for 250 nA).

TABLE 11. AVERAGE OF ALMA 480 CURRENT TESTS FOR 10 NEUTRON IRRADIATED TRANSMITTERS

TRANSMITTER No. *AVG*	DATE: LEVEL:	5/30 Pre RAD	6/1 $5x10^{12}$	6/6 $1x10^{13}$	6/8 $4x10^{13}$	6/12 $7x10^{13}$	6/13 $1x10^{14}$	6/14 $4x10^{14}$	6/27 $7x10^{14}$
I_d - 50mA	(mA)	50.380	50.310	50.280	50.180	49.860	49.540	48.190	46.130
I_d - 75mA	(mA)	74.850	74.780	74.630	74.410	74.110	73.620	71.420	68.050
I_d - 25mA	(mA)	25.450	25.460	25.470	25.340	25.210	25.040	24.380	23.460
I_d - 150mA	(mA)	147.250	147.250	146.830	145.990	144.410	143.840	140.680	132.230
I_d - off	(μA)	2.277	2.305	2.451	2.340	2.260	2.229	2.131	2.045
I_{cc}	(mA)	31.940	30.190	31.940	31.830	31.640	31.500	30.690	29.470
I_{IL} - PIN 10	(mA)	-1.109	-1.108	-1.109	-1.104	-1.101	-1.095	-1.079	-1.039
I_{IH} - PIN 11	(μA)	0.042	0.080	0.159	0.102	0.034	0.024	0.017	0.029
I_{IL} - PIN 11	(mA)	-1.109	-1.107	-1.107	-1.104	-1.099	-1.093	-1.073	-1.031
I_{IH} - PIN 10	(μA)	0.366	0.404	0.486	0.424	0.347	0.321	0.313	0.319

TABLE 12. TRANSMITTER CURRENT VARIATIONS AS MEASURED BY RECEIVER PHOTODIODE CURRENT (nA) VERSUS NEUTRON FLUENCE (n/cm^2)

DEVICE NO.	PRE	$5x10^{12}$	10^{13}	$4x10^{13}$	$7x10^{13}$	10^{14}	$4x10^{14}$	$7x10^{14}$
10	285	285	280	285	280	280	270	255
11	260	260	250	260	255	250	240	230
12	290	290	290	295	295	285	275	260
13	275	280	280	280	280	280	260	250
14	260	260	260	270	270	265	255	245
15	275	280	275	285	280	275	265	255
16	280	285	285	290	290	285	270	260
17	285	280	280	285	280	280	265	250
18	285	280	285	285	280	280	270	250
20	290	290	295	295	290	285	275	260

The transmitter LED drive current appears very uniform up through 1×10^{14} n/cm^2. At 4×10^{14} and 7×10^{14} n/cm^2 the transistor LED current begins to decrease as seen by the corresponding decrease in photodiode current. At 7×10^{14} n/cm^2 the photodiode current has decreased by 10 percent which is very similar to the LED current drive decrease seen by the transmitters at higher LED currents (ALMA 480 tests).

DOSE RATE TESTS

Radiation testing was conducted on three receivers and three transmitters at AFWL's Febetron 705 Flash X-ray (FXR) machine (20 ns pulse width). Upset levels were determined for (a) the entire fiber optic system being exposed (including the LED, fiber, and photodiode); (b) only the transmitter exposed; and (c) only the receiver exposed. The objective was to measure the upset levels at a variety of photodiode current levels.

During test setup and checkout in the FXR screen room, the problem of obtaining bit errors caused by electrical activity (plugging equipment into AC outlet, turning lights or equipment on or off, etc.) persisted. Since it was anticipated that firing of the FXR machine would cause a similar situation, elimination of the problem appeared necessary to obtain upset level data. By increasing the LED current, which increased the photodiode current to 1 μA, and by obtaining AC power for all instrumentation and equipment from a different shielded screen room via extension cords, the problem of electrical

noise simulated bit errors appeared solved. The next step was to fire some FXR test shots with the entire fiber optic system well shielded. Firing of the FXR machine still caused unwanted bit errors even after the apparent fix. Until this point, attenuation of the fiber optic signal seen at the photodiode receiver was controlled by reducing the LED drive current with a variable resistor tied to the transmitter's output transistor emitter. Increasing the LED current to 150 mA and optically attenuating the signal did not have any effect on the unwanted errors. Since the FXR shot is a single predictable event, it was a good source to trigger an oscilloscope and observe what signals were causing the bit errors. Figure 6 (a-d) shows FORIC output waveforms at different current levels and other critical signals with the system still completely shielded (the FXR pulse occurs 500 ns after the start of the trace sweep). Besides the output errors, the only other signal that looked faulty was the receiver preamp output which causes the erroneous output. The only short-term solution found was to increase the photodiode current up to 10 μA where a good response is obtained (Fig. 6d).

The transmitter was tested for upset by covering the remainder of the 20 x 30 cm fiber optic system box with 2-inch lead bricks and leaving a 1 x 2.5 cm opening for the transmitter IC. The upset level for the transmitter was found to be independent of the LED current magnitude. Th highest dose rate obtainable with all the shielding around the rest of the circuit was 3.8×10^9 rads/s. Figure 7 shows the results at this distance which just happened to be the minimal upset level. The LED current (Id) was varied from 2 μA to 150 μA (photodiode current varied from 0.5 μA to 40 μA). The main difference between the photographs appears in the number of bit errors recorded from the receiver output which does vary with input current. At a dose rate of 1.5×10^9 rads/s, The LED current exhibited some minor waveshape degradation at the time of the pulse. At 8.8×10^8 rads/s there was no indication at all of any upset. All three transmitters exhibited similar characteristics and upset levels. ALMA 480 tests were identical on these devices before and after dose rate testing.

The minimum upset levels for the receivers were fairly low. The responses are shown in Figure 8 and summarized in Table 13.

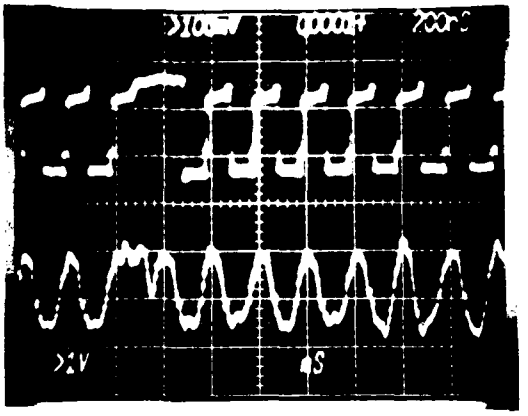

Figure 6a. Photodiode set at 2uA.
Top trace: FORIC output
Bottom: FORIC pre amp

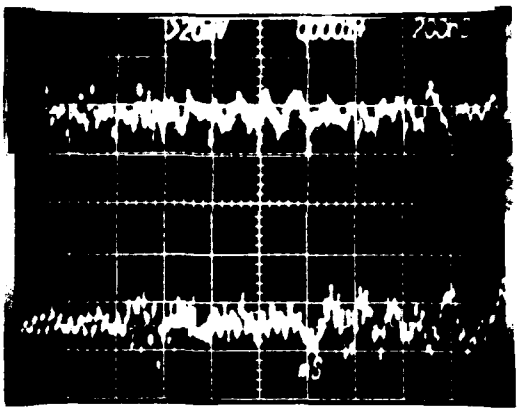

Figure 6b. Photodiode set at 2 uA.
Top trace: FORIC Vcc
Bottom: Photodiode reverse bias (V_r = 40v)

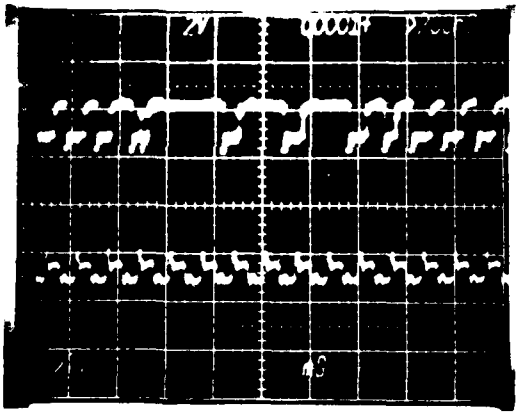

Figure 6c. Photodiode set at 300nA
Top trace: FORIC output
Bottom: FOTIC LED current

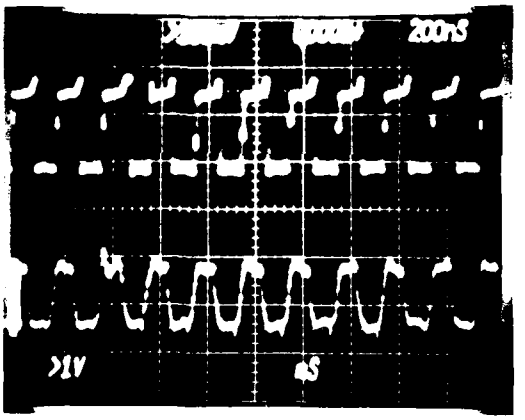

Figure 6d. Photodiode current - 10 uA
Top trace: FORIC output
Bottom: FORIC pre amp

There was no exposure at the test box in these tests. The disturbances seen come from electrical noise of the burst. The larger the photodiode current, the better the output response. The burst occurs 500 ns after start of the trace.

Figure 6. FXR Electrical Noise Induced Upsets with the Test Box Totally Shielded.

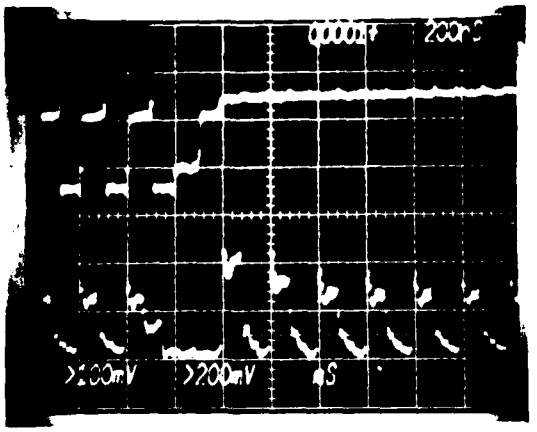

Figure 7a. Photodiode set at 0.5 uA
LED current - 2 mA
FORIC output has 20 errors

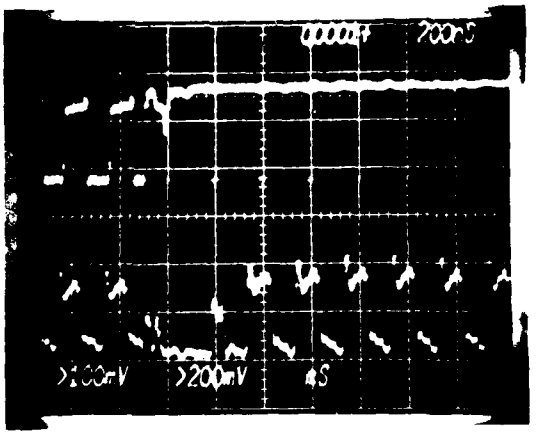

Figure 7b. Photodiode set at 2.0 uA
LED current - 8 mA
FORIC output has 12 errors

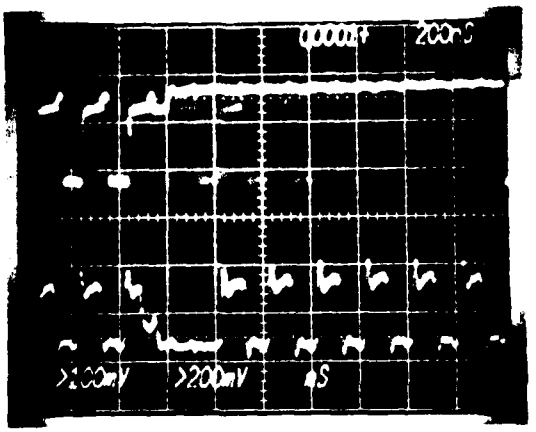

Figure 7c. Photodiode set at 10 uA
LED current - 40 mA
FORIC output has 8 errors

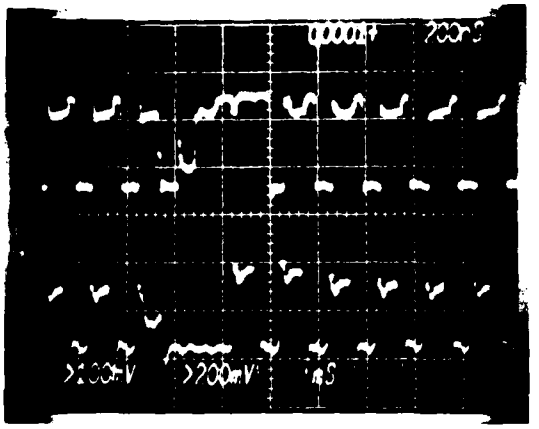

Figure 7d. Photodiode set at 40 uA
LED current - 150 mA
Foric output has 1 error

All photographs have the transmitter unshielded. The dose rate is 3.8×10^9 rads/sec. The top trace of each picture is the FORIC output and the bottom is the FOTIC LED output (pin 4). The FOTIC output upset is seen to be independent of LED current. The FORIC bit errors are measured by the error detection circuit.

Figure 7. Transmitter Transient Radiation Tests

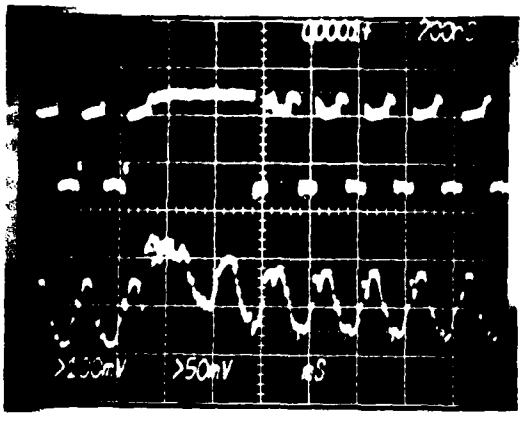

Figure 8a. Dose rate 4.5×10^6 rads/sec
Photdiode current - 2 uA

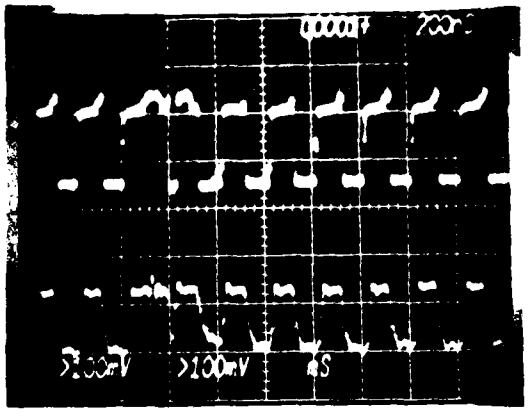

Figure 8b. Dose rate: 6.7×10^6
Photodiode current - 10uA

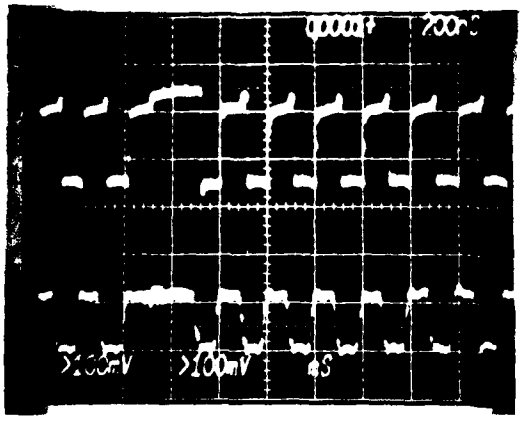

Figure 8c. Dose rate: 1.5×10^7 rads/sec
Photodiode current - 40 uA

Minimum receiver upset levels at various photodiode currents.

The top trace in all photographs is the FORIC output and the bottom trace is the FORIC pre amp output. These tests were performed with only the receiver being irradiated. The pulse occurs 500 ns after the start of the sweep. The larger the photodiode current, the better the radiation response.

Figure 8. Receiver Transient Radiation Tests.

TABLE 13. RECEIVER UPSET LEVELS

PHOTODIODE CURRENT (I_I) LEVEL	UPSET (rads(Si)/s) LEVEL
40 μA	1.5×10^7
10 μA	6.7×10^6
2 μA	approx. $3\text{-}4 \times 10^6$

TABLE 14. MINIMUM OPERATING CURRENT BEFORE AND AFTER FXR TESTS

RECEIVER NO.	MINIMUM CURRENT (nA)	
	PRE FXR	POST FXR
19	240	240
27	350	350
28	300	305

The upset level at 2 μA photodiode current is approximate because at such low current levels the FXR machine noise causes faulty outputs as stated earlier. This made it difficult to determine a precise value for upset level. All three receivers had similar upset levels and experienced no changes in minimum current or bit error rates. To determine the receiver recovery time, the test box was moved as close as possible to give a larger dose rate while still shielding all but the receiver. Figure 9 shows that at the maximum rate of 9×10^8 rads/s the receiver output goes high for 3 μs then drops to a low state for 55 μs before the preamp signal (pin 9) regains some amplitude and the output comes back.

The final sequence of dose rate tests was done with the whole system exposed. As expected, failures resulted all the way to the minimum dose-rate obtainable without shielding. Figure 10 shows the system response at 5×10^6 rads/s. The error detector recorded three errors at 40 μA at this dose rate. There was only a small difference between the 2 μA and 10 μA test. Although the preamp output looks like the same amplitude during all the dose rate tests for all current levels, the amplitude does increase as the photodiode current increases. The oscilloscope traces were adjusted to give uniform preamp output pulses.

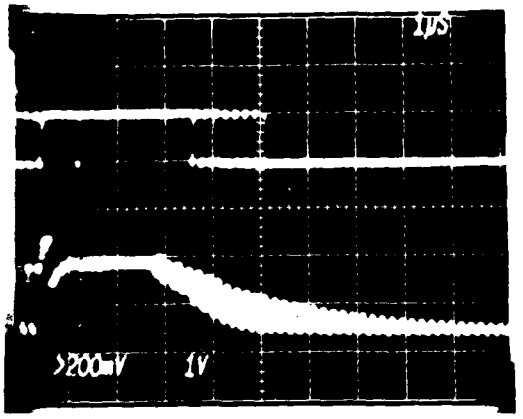

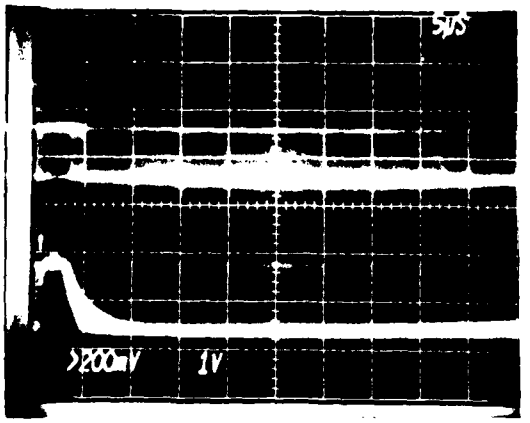

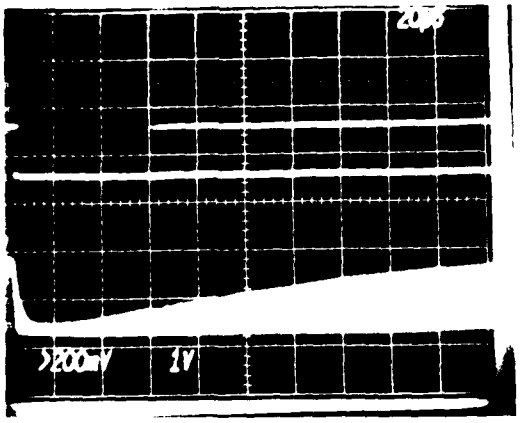

Figure 9. Receiver recovery time following a burst a $9x10^8$ rads/sec.

The above traces show the response of the receiver biased at 10 uA photodiode current to a $9x10^8$ rads/sec pulse at different increments of time. The top trace is the FORIC output and the bottom trace is the pre amp output. Recovery of the FORIC output occurs 55 us after the pulse. A dose rate of $9x10^8$ is the maximum obtainable when shielding the total circuit except for the receiver.

Figure 9. Receiver Recovery Time Following a $9x10^8$ Rad/s Burst.

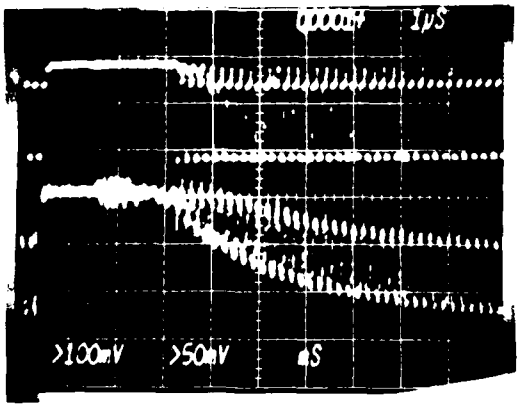

Figure 10a. 2uA photodiode current FORIC output has 16 errors

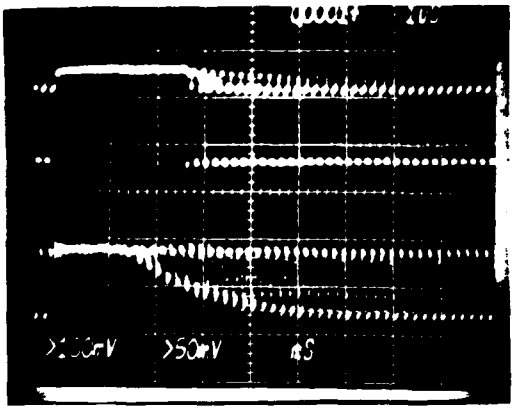

Figure 10b. 10uA photodiode current FORIC output has 15 errors

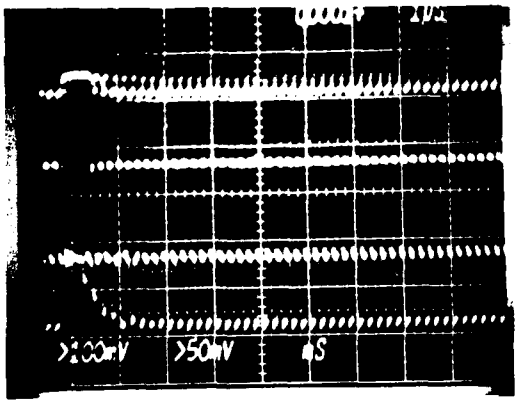

Figure 10c. 40uA photodiode current FORIC output has 3 errors

Upset level for the entire fiber optic system exposed.

The photographs show the FORIC output response (top trace) and the pre amp output (bottom trace) for the entire system exposed at 5×10^6 rads/sec. This is the minimum dose rate obtainable. The output errors were measured by the error detection circuit.

Figure 10. Transient Upset for the Entire Fiber Optic System Exposed.

IV. CONCLUSIONS (SPX 3619, SPX 3620)

The receiver and the transmitters performed satisfactorily in a Co-60 total ionizing dose environment up to 5 Mrad(Si). Transmitter 7 did unexpectedly show problems in the 1-5 krad range, but due to the very consistent response through the rest of the radiation tests, it is not likely that radiation was the cause of the damage. There were no significant differences in devices that were irradiated passively, biased, or biased with clocked inputs. At 5 Mrad, the transmitter current degraded 5 percent and the receiver sensitivity actually improved. No devices had a BER larger than 10^{-8} bit errors/s.

The neutron tests showed that the transmitters worked fine through 7×10^{14} n/cm^2. The transmitter currents were beginning to degrade at 4×10^{14} n/cm^2, and were down 13 percent of the preirradiation levels at 7×10^{14} n/cm^2. The sensitivity of most receivers increased 20 percent at 4×10^{14} n/cm^2, but at 7×10^{14} n/cm^2 the photocurrent required for operation increased an order of magnitude to 2-5 μA. To insure reasonably low minimum operating currents, the passively irradiated receivers should not be exposed to more than 4×10^{14} n/cm^2.

In a dose rate environment, the transmitter upset threshold is about 1.5×10^9 rads/s. This level is independent of the LED current (within the tested range of 2 μA to 150 μA). At 40 μA photodiode current (using maximum LED current) the receiver upset level is 1.5×10^7 rads/s. At 2 μA the upset level is approximately 3.5×10^6 rads/s. Lower photodiode current upset levels could not be tested in this environment due to severe electrical noise induced upsets. At 1×10^9 rads/s with a 10 μA photodiode current, recovery time following the burst is approximately 60 μs (worse for lower photodiode current levels). For total system exposure, the system upset level would be below 10^6 rads/s at low photodiode receiver currents.

V. ELECTRICAL TESTING (SPX 4125, SPX 4126)

This section describes the electrical tests performed on the fiber optic transmitter and receiver modules. These tests were performed before irradiation and after each incremental level of total gamma dose and total neutron fluence.

No major changes in any of the test fixtures or procedures were necessary from the writing of the test plan. Any changes that were made are noted in the general procedure descriptions following:

TRANSMITTER PARAMETRIC TESTS

Several of the transmitter tests were performed under static conditions. These included the worst case power supply current measurements and the worst case input current measurements. These tests were performed manually on an ALMA 480 integrated circuit tester.

The balance of the tests were performed with the transmitter in an active operational mode. The general fiber optic system configuration is given in Figure 11. All tests, in which the transmitter was actively operating, were performed using a receiver designated as a control device. A device designated as a control device is not subjected to any radiation environment at all. This was done to insure that any system degradation is due solely to the irradiated device.

The active tests are done using a 5 MHz square wave input signal. The measurements include the system propagation delay and an optical output power measurement. The propagation delay is measured at a photodiode bias of +5 V and +30 V. The irradiated transmitter's average optical output power was compared to that of a control transmitter to determine any optical output degradation. This was accomplished by adjusting the optical output of the control device to a given level (1. 26 μW) which was the same throughout testing. After this level is set, the control device is removed from the circuit (without changing anything else) and is replaced by the irradiated device. The resulting power readings form an output power ratio. This ratio is then normalized with respect to the power ratio at zero rads(Si). This reflects a percentage change in the optical output power level.

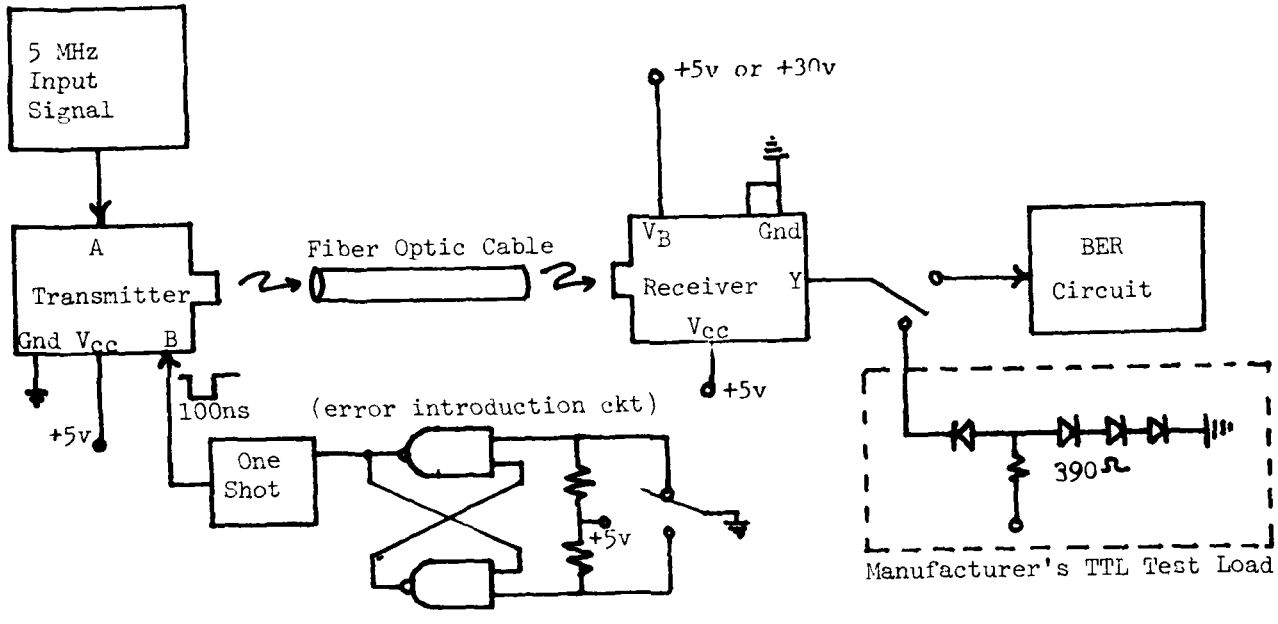

Components

Transmitter	Spectronics SPX 4125
Receiver	Spectronics SPX 4126
Fiber Optic Cable	Galite 3000
Load Diodes	1N914 (or equivalents)

Figure 11. Fiber optic system under test configuration

The method for obtaining variability (attenuation) of the optical output power will be briefly described. The fiber optic output cable is coupled to another fiber optic cable across a variable distance. The attenuation can be varied by changing the distance separating the two cables. Optical filters were originally to be used to achieve the attenuation but the coupling losses alone were enough to achieve our purpose. The variable distance configuration also gave more flexibility in the amount of attenuation. The optical power measurements were made using an optical power meter.

RECEIVER PARAMETRIC TESTS

All of the receiver tests were done during active operation using a 5 MHz square wave input signal.

The measurements included the propagation delay between the system's input and output voltage waveforms. The rise and fall times of the output waveform and the power supply current during normal operation were also measured. The delay time measurements were made using the manufacturer's TTL test load circuit (Figure 11), so that direct comparison of data is possible. The power supply current measurements were done with the BER circuit as the load. Throughout testing this loading drew about 3 mA more current than the manufacturer's test load. Thus, it represented a worse case value. All of the measurements were done at a photodiode bias of +5 V and +30 V.

Two input conditions were imposed on the receivers. First, all of the receivers were tested at a specified input optical power level (2.52 μW), which was the same throughout testing. The second condition was established by attenuating the input signal to slightly above the operating threshold of the test receiver. All of the measurements described above were taken at both of these power levels.

RECEIVER FUNCTIONAL TEST - BIT ERROR RATE (BER)

The BER is expressed in errors per pulse and is the chance of an error occurring during the time interval associated with that pulse.

A block diagram of the general fiber optic test circuit, which includes the BER test circuit, is shown in Figure 12. A simplified timing diagram is presented in Figure 13.

The operation of the BER circuit is straightforward. The 5 MHz square wave input to the fiber optic system under test is also applied to a set of hex inverters. These inverters are used to delay the signal until this simulated signal closely matches the actual fiber optic system's output, as seen on an oscilloscope (hex inverters were used instead of hex buffers due to chip availability). These two signals are applied to the address lines of a multiplexer where the actual comparison is accomplished. The multiplexer inputs are in states such that when the multiplexer is enabled, a positive pulse is output if an error is present. Cleaner outputs were obtained by using one of the multiplexers on the chip for the zero comparison, two strobe (enable) pulses are generated by edge triggered multivibrators. The first set of multivibrators is triggered from the simulated fiber optic waveform. They have adjustable pulse widths and are used to position the second set of multivibrators as near as possible to the center of the highs and lows of the simulated waveform. The second set prduces the actual strobe pulses which are 45 ns long. One strobe enables multiplexer one on the highs and the other strobe enables multiplexer two on the lows. All of these signals are closely monitored on a dual beam oscilloscope. If an error is present a 45 ns positive pulse is presented to an OR gate, which passes it to the counting circuitry. If the fiber optic output should have been a zero, but was not, a flip-flop is set to drive LED 1. If the decade counters count more than 99 errors, another flip-flop is set driving LED 2.

An error introduction circuit was added to the circuitry to make sure the BER circuitry was operating properly (for a detailed drawing, see Figure 11). A one-shot multivibrator was connected to input B of the transmitter. This point is normally high, enabling the transmitter to function properly. A debounced switch is used to enable a one shot which holds input B low for approximately 100 ns. This introduces at least one error which should be updated on the BER circuit.

For efficient operation of these fiber optic devices, transmitted data should be Manchester encoded. The necessary circuitry for such a code was not developed, as it was recognized that a 5 MHz square wave is equivalent to a 5 Mbit/s data rate of all ZEROS or ONES. Since it was only necessary to functionally exercise the devices during testing, this was a perfectly acceptable input. It should be noted that all ZEROS and ONES is the best case input to these devices.

VI. RADIATION TEST RESULTS (SPX 4125, SPX 4126)

TOTAL GAMMA DOSE TESTS

Total dose testing was performed at AFWL's 5 kCi Co-60 facility on two transmitter/receiver pairs. The devices were electrically evaluated after 50, 100, 300, 500, and 700 krads, 1, 2, and 3 Mrads(Si) of total gamma dose was absorbed. One transmitter/receiver pair was passively irradiated with all of the device pins grounded. The other pair was actively operated during the testing using a 1 MHz square wave input. This pair was butted together and aligned so that operation of the devices was possible. This type of placement gave a more uniform radiation exposure over both devices, and irradiating a fiber optic cable was not necessary. The photodiode was operated with +5 V bias and the system output was monitored on an oscilloscope.

Before presentation of the test data, a table (Table 15) will be presented that gives the manufacturer's maximum specifications. Because of the modular construction of the devices, the propagation delay and rise time measurements are total system measurements. The maximum system times were computed using the square root of the sum of the squares of each component's maximum time. The rise time of the cable was neglected because of its small material constants (multimode dispersion, 22 ns/km; material dispersion 3.5 ns/km), and the short length of cable used (less than 1.5 m).

The transmitter data is presented in Tables 16 through 19. Table 16 contains the calculated power ratio percentages. The table entries are determined by dividing the test device's optical output power by the reference device's output power (which was constant throughout testing). This ratio is then divided by the respective preirradiation ratio. This then gives a direct means in which to see the percentage change in the optical output power.

Throughout the data presentation, the PASSIVE subscript (or title) refers to the devices irradiated with all pins grounded. The ACTIVE subscript (or title) refers to the device pair that was actively operated during irradiation.

Except for an unexpected gain seen in the 300-500 krad(Si) range, the transmitter's efficiency decreases with total dose to finally show a 28% loss by the 3 Mrad(Si) irradiaton.

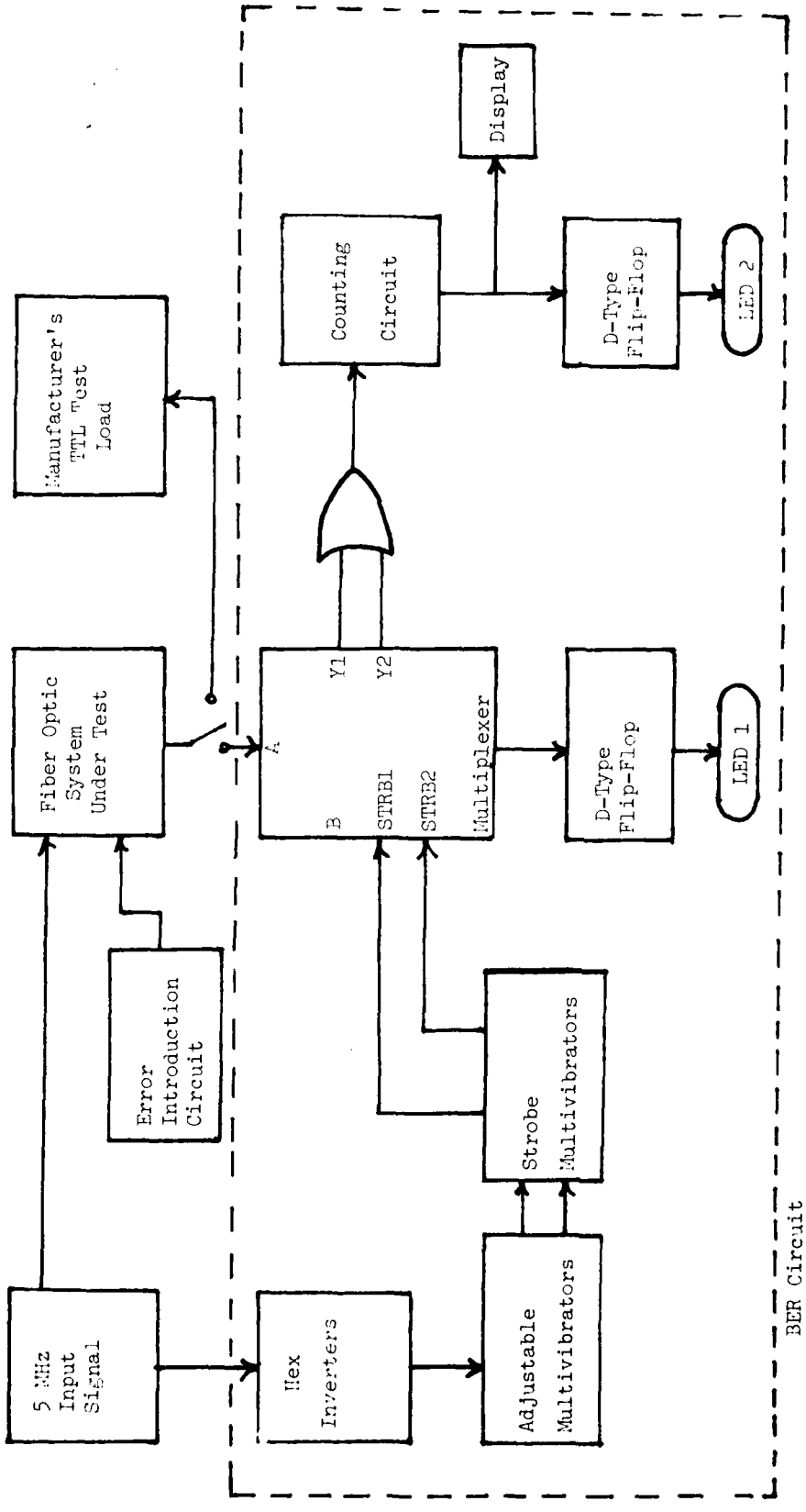

Figure 12. General Fiber Optic Test Circuit (including BER circuit)

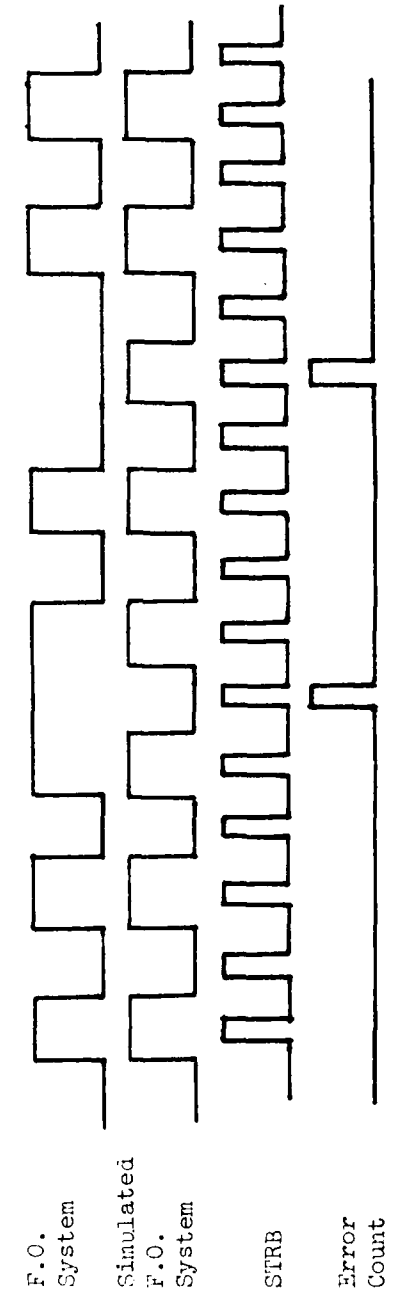

Figure 13. Timing Diagram for BER Circuit

TABLE 15. MANUFACTURER'S MAXIMUM RATINGS

DEVICE	PARAMETER	SYMBOL	TYP	MAX	UNITS
Transmitter	Input High Level Current	I_{IH} [1]	1	40	μA
	Input Low Level Current	I_{IL} [2]	-1.2	-1.6	mA
	High Level Supply Current	I_{CCH} [3]	119	135	mA
	Low Level Supply Current	I_{CCL} [4]	28	35	mA
Receiver	Supply Current	I_{CC}	48	55	mA
	Minimum Optical Input Power	P_m	700		nW
System	Propagation Delay Low-High	$t_{D(L-H)}$	31	51	ns
	High-Low	$t_{D(H-L)}$	31	51	ns
	Output Transition Time Low-High	t_r	8	14.1	ns
	High-Low	t_f	3	12.2	ns
	Pulse Width Distortion	$t_{D(L-H)} - t_{D(H-L)}$	0	7.6	ns

[a] Input not under test is at ground.

[b] Input not under test is a 2.4 V.

[c] Both inputs at 2.4 V.

[d] One input is at 0.4 V, the other is at either 0.4 V or 2.4 V.

TABLE 16. NORMALIZED OPTICAL OUTPUT POWER RATIO (Φ) VS. TOTAL DOSE (γ_D)

γ_D (rads (Si))	$\Phi_{Passive}$	Φ_{Active}
0	1.00	1.00
50 K	0.89	0.94
100 K	0.86	0.87
300 K	0.87	0.97
500 K	0.88	0.88
700 K		0.81
1 M		0.82
2 M		0.75
3 M		0.72

TABLE 17. POWER SUPPLY CURRENT VS. TOTAL GAMMA DOSE

γ_D(rads (Si))	PASSIVE		ACTIVE	
	I_{CCH}(ma)	I_{CCL}(ma)	I_{CCH}(ma)	I_{CCL}(ma)
0	117.9	29.5	123.4	29.5
50 K	117.5	29.4	123.1	29.4
100 K	116.8	29.1	122.8	29.1
300 K	115.5	28.9	122.3	29.1
500 K	114.8	28.6	122.1	28.8
700 K			121.9	28.7
1 M			121.9	28.8
2 M			122.3	28.6
3 M			122.8	28.7

TABLE 18. TRANSMITTER INPUT CURRENT VS. TOTAL GAMMA DOSE

γ_D(rads(Si))	PASSIVE		ACTIVE	
	I_{IL}(ma)	I_{IH}(na)	I_{IL}(ma)	I_{IH}(na)
0	-0.988	10	-0.958	13
50 K	-0.982	10	-0.948	14
100 K	-0.982	7	-0.952	8
300 K	-0.965	7	-0.926	10
500 K	-0.963	5	-0.926	7
700 K			-0.895	7
1 M			-0.912	7
2 M			-0.907	6
3 M			-0.898	6

TABLE 19. TRANSMITTER PROPAGATION DELAY VS. TOTAL GAMMA DOSE

γ_D(rads(Si))	PASSIVE		ACTIVE	
	$t_{D(L-H)}$(ns)	$t_{D(H-L)}$(ns)	$t_{D(L-H)}$(ns)	$t_{D(H-L)}$(ns)
0	58	58	58.5	59
50 K	59	61	61	60
100 K	60	57	61	60
300 K	53	67	54	71
500 K	52	67	54	71
700 K			54	71
1 M			50	70
2 M			50	69
3 M			61	61

The PASSIVE transmitter failed before the 700 krad(Si) evaluation. The failure, however, did not seem to be radiation induced but rather a reliability problem. The high level power supply current rose approximately 50 mA. The low level supply current rose by 20 mA. The input current levels seemed to imply input B was held low, but the device could be operated by switching input A, implying B was held high. The output power ratio rose to approximately 1.6, indicating a 72% increase in the optical output signal. It would seem most of the excess power supply current was being pumped into the LED.

The transmitter power supply current measurements are presented in Table 17, and the input current measurements are presented in Table 18. The power supply current remains essentially constant throughout the testing (no more than 3% variance). Until the very high doses are obtained, the trend seems to be a lessening of this requirement. At no time does it come near the manufacturer's maximum specification.

There was no significant difference between data taken on input A versus input B. Therefore, only the data for input A is presented (for input B data, see Appendix C). When the input high level current was measured, the input not under test was held at + 0.4 V instead of ground as was done by the manufacturer. This was an oversight, but it affects the data very little. Subsequent input high tests, with the input not under test grounded, approximately doubled the current level. This appears to be a large increase, but these levels are still in the 20 nA range while the devices have a maximum specification of 1 μA.

Table 19 gives the transmitter propagation delay data.

The data presented were taken with a photodiode bias of +5 V. Data were also taken at a +30 V bias. The only difference this made throughout testing was to decrease the delay times 3-5 ns at the +30 V bias.

Note that the propagation delay data do not follow any expected pattern. There are changes in the middle dose ranges that disappear in the high dose range, so that the net change beginning to end is less than 3%. There is up to a 20% variance in the mid-dose range. This almost random data pattern would seem to suggest some instability in our measurement technique. However, intensive preirradiation evaluation produced variances of less than 3% - 5%. During the actual testing, repeated insertion of the device under test into the test circuit produced variances of negligible significance. The calculated

maximum specification for delay time was excluded from the beginning.

Tables 20 through 24 contain the data for the receiver tests. Figure 14 is a graphical presentation of the minimum optical input power necessary to operate the receiver.

The minimum power required for receiver operation follows an interesting pattern. The efficiency of the photodiode appears to increase initially. Then there is a large increase in the necessary optical input power followed by a period of recovery. While the passively irradiated device continues to show a decrease in the minimum operational power, the actively operated device begins a definite increase in the necessary input power. It finally shows an increased need of 140% over the preirradiation level. The passive device shows a 12% decrease in te necessary optical input power. The actively operated device fails to meet the manufacturer's specification of 700 nW as being the minimum power for operation for any dose above 300 krad(Si). The 50 krad data were thrown out because an error in the data acquistion method was discovered.

The receiver power supply current changed over a 25% range. It initially increases with total dose, but then shows improvement in the higher doses. The maximum rating was never exceeded, but it was close in the middle dose range.

The receiver propagation delay measurements are much the same as the transmitters. The same question again arose, but the same justification for the readings being accurate is put forth. Again the manufacturer's maximum rating was exceeded by even the nonirradiated devices. The pulse width distortion becomes exceedingly large (15 ns) and then returns to within specifications (7 ns). This is caused by the initial gradual decrease of the low to high delay and an increase in the high to low delay. This deterioration is reversed in the high dose range. Only the data taken at a photodiode bias of +5 V are presented. Data taken at +30 V follow the same pattern but are consistently 3-5 ns faster (for +30 V bias data, see Appendix C).

The risetime measurements were generally slower when the receiver was operated at the minimum power for operation and at a photodiode bias of +5 V (the +5 V bias data are in Appendix C). There was a sudden sharp improvement in the active device after the 3 Mrad(Si) exposure.

TABLE 20. MINIMUM POWER FOR OPERATION (P_m) VS. TOTAL GAMMA DOSE

γ_D(rads(Si))	$P_{m(Passive)}$ (μW)	$P_{m(Active)}$ (μW)
0	0.568	0.643
50 K	-	-
100 K	0.510	0.499
300 K	0.504	1.414
500 K	0.915	1.15
700 K	0.638	1.19
1 M	0.638	1.32
2 M	0.514	1.35
3 M	0.499	1.52

TABLE 21. RECEIVER POWER SUPPLY CURRENT VS. TOTAL GAMMA DOSE

γ_D(rads(Si))	PASSIVE		ACTIVE	
	I_H(ma) [1]	I_M(ma) [2]	I_H(ma)	I_M(ma)
0	48.5	44.0	39.5	39.4
50 K	49.0	47.8	43.0	43.6
100 K	47.5	48.5	44.3	45.0
300 K	53.7	54.8	48.8	49.0
500 K	54.0	55.0	49.0	48.8
700 K	53.8	53.5	48.8	48.6
1 M	53.8	53.4	48.8	48.6
2 M	49.1	49.0	45.3	45.6
3 M	46.7	46.7	42.9	42.8

[a] I_H is measured when the optical input power to the receiver is 2.52 μW.

[b] I_M is measured when the optical input power to the receiver is the minimum to permit operation.

TABLE 22. RECEIVER PROPAGATION DELAY (FOR V_B = 5 V, P = MINIMUM FOR OPERATION) VS. TOTAL GAMMA DOSE

γ_D(rads(Si))	PASSIVE		ACTIVE	
	$t_{D(L-H)}$(ns)	$t_{D(H-L)}$(ns)	$t_{D(L-H)}$(ns)	$t_{D(H-L)}$(ns)
0	60	60	63	62
50 K	61	59	64	62
100 K	63	61	67	63
300 K	58	70	56	71
500 K	56	71	58	78
700 K	58	71	58	77
1 M	58	71	59	76
2 M	59	70	61	74
3 M	65	58	65	64

TABLE 23. RECEIVER PROPAGATION DELAY (FOR V_B = 5 V, P = 2.52 μW) VS. TOTAL GAMMA DOSE

γ_D(rads(Si))	PASSIVE		ACTIVE	
	$t_{D(L-H)}$(ns)	$t_{D(H-L)}$(ns)	$t_{D(L-H)}$(ns)	$t_{D(H-L)}$(ns)
0	56	57	55	61
50 K	56	57	58	57
100 K	57	55	57	60
300 K	52	65	58	70
500 K	50	68	56	71
700 K	50	67	58	71
1 M	50	68	58	71
2 M	49	68	58	69
3 M	59	58	59	61

TABLE 24. RECEIVER RISE TIME (V_B = 30 V) VS TOTAL DOSE

γ_D(rads(Si))	PASSIVE		ACTIVE	
	t_{rH}(ns)[1]	t_{rL}(ns)[2]	t_{rH}(ns)	t_{rL}(ns)
0	5.5	6	11	11.5
50 K	6.5	6	11	11
100 K	7	8	13	12
300 K	7	11	13.5	13
500 K	6.5	12	11	16
700 K	6	10	11	14
1 M	6	11	12	15
2 M	7	10	12.5	17
3 M	8	9	11.5	11

[a] t_{rH} refers to the rise time with input power equal 2.52 μW.

[b] t_{rL} refers to the rise time with input power equal to the minimum power necessary to drive the receiver.

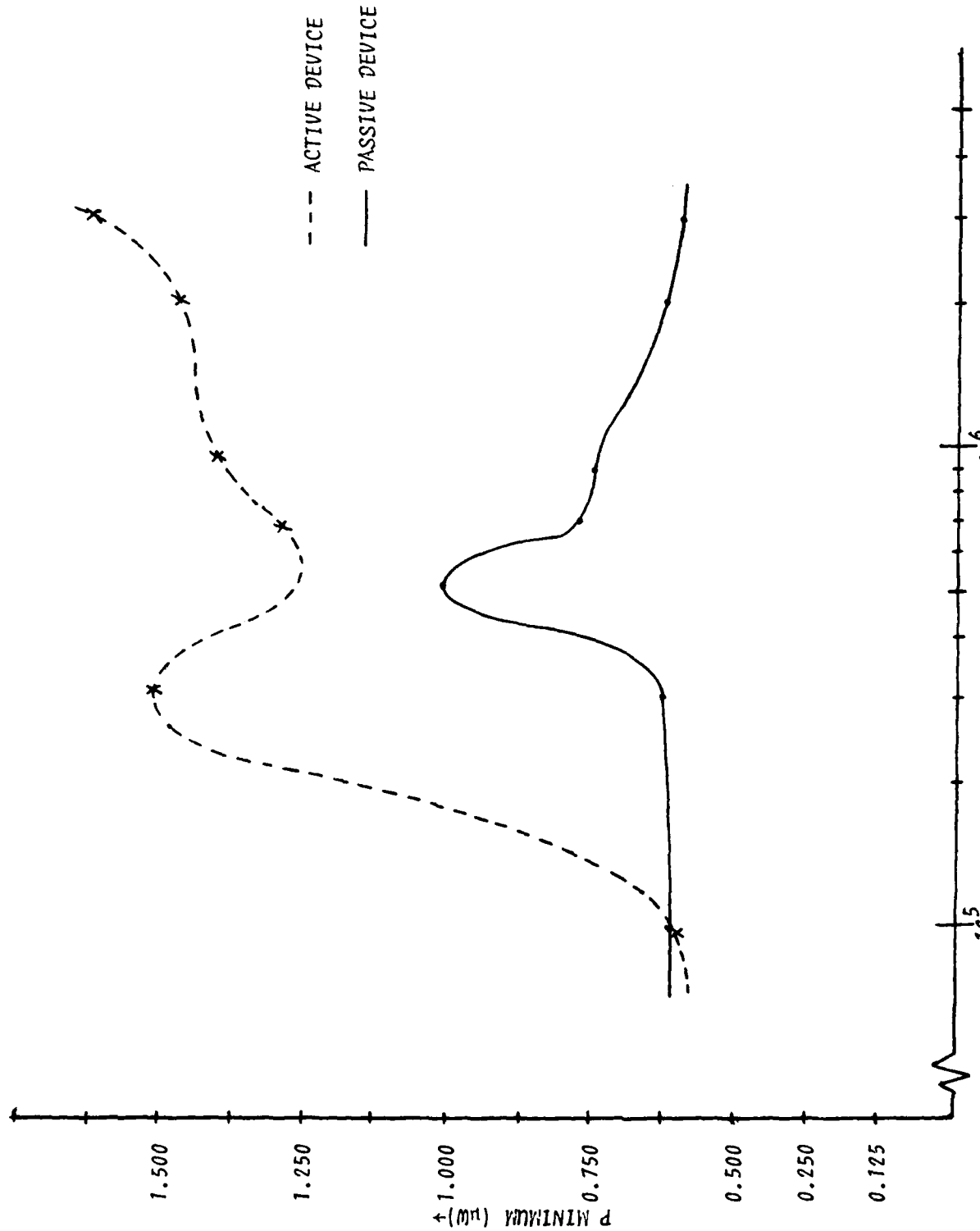

Figure 14. Receiver minimum power for operation vs. total gamma dose.

The fall time data are not presented here because, during testing in any configuration, the fall time remained essentially constant at 3 ns. The largest increase was from 2.5 ns to 4 ns. This is well below the maximum specification (fall time data are in Appendix C).

Throughout testing the BER measurement was performed at the minimum power for operation and at a photodiode bias of +5 V. The only errors ever recorded occurred after the 3 Mrad(Si) exposure of the passive device (two errors counted). All of the other events were zero. In the 16½ minutes of the test, approximately 100 errors would have had to occur to exceed the manufacturer's rated BER of 10^{-8} bits/s. The data collected indicate a BER of approximately 10^{-10}.

DOSE-RATE TESTS

The dose rate testing was performed at AFWL's Febetron 705 flash X-ray machine (20 ns pulse width). One transmitter/receiver pair was evaluated in this environment. The devices were electrically evaluated, as in Section V, before and after the dose rate testing. These evaluations showed no changes.

Before the actual device tests began, an experiment was performed to evaluate the shielding obtained from the metal module. Dosimetry measurements were performed on a hollowed out module. These measurements indicated that the module reduced the dose rate by about 12%. All of the dose rates given with the data do not take this into account. To obtain the actual dose rate absorbed by the electronics, 12% of the given dose rate must be discounted.

The receiver responses are shown in Figure 15. The receiver tests were done by shielding the 8- x 12-inch test box with 5-cm lead bricks, having only a 1- x 1-cm opening in front of the receiver. The minimum upset level was so low that the opening had to be covered with lead. Pieces of lead 1/8-inch thick were placed one at a time in front of the opening until the dose rate was low enough for minimum upset. Minimum upset was defined to be when the dose rate caused only one error. The dose levels became so low as to be unmeasurable on the equipment available to us and could only be approximated.

The minimum upset level was dependent upon the optical input power. With everything at the optimum operational level (i.e., maximum input power, photodiode bias of +30 V), the minimum upset level was 1.3×10^6 rads/s. Minimum upset occurred at much lower dose rates if the optical input power was decreased.

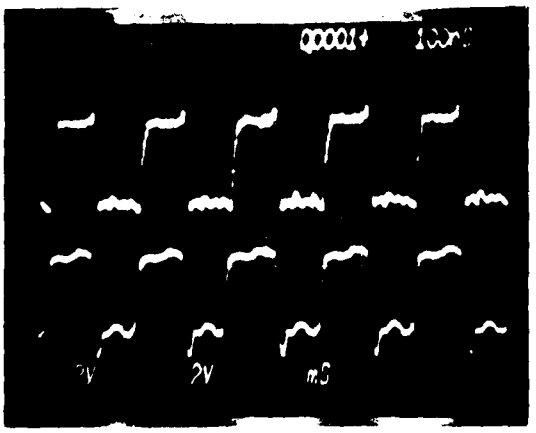

(a) "0" test, all circuitry well shielded.

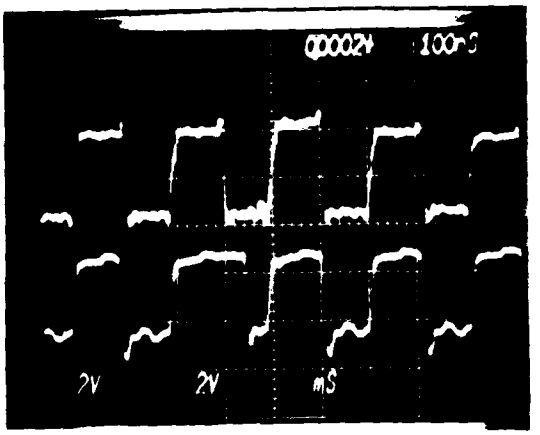

(b) Dose rate: 1.3×10^6 rads/s
Optical power: 32μW

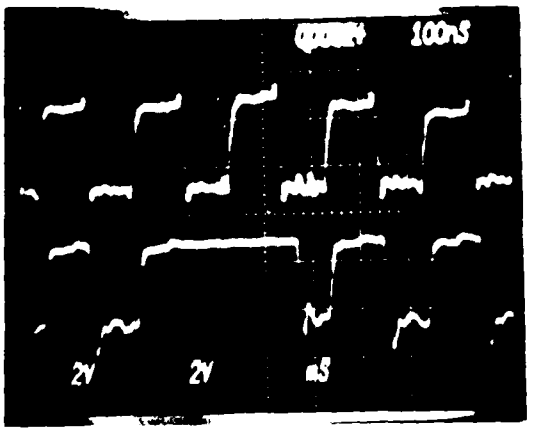

(c) Dose rate: 7.6×10^5 rads/s
Optical power: 5.5μW

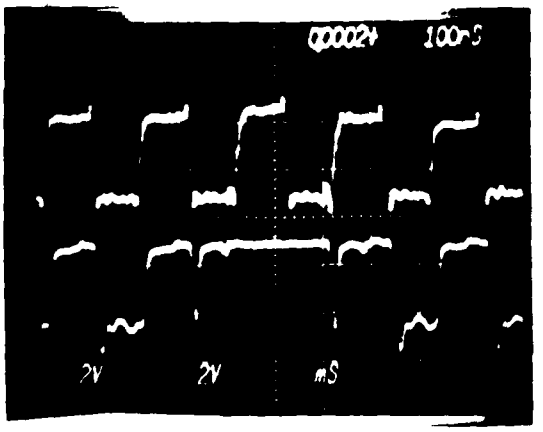

(d) Dose rate: 10^5 rads/s
Optical power: 2.5μW

The top trace in all photos is the input to the fiber optic transmitter and the bottom trace is the receiver output. The pulse occurs approximately 350ns after the start of the trace.

Figure 15. Receiver Minimum Upset Levels With Varying Optical Input Power

Changing the photodiode bias from 30 V to 5 V caused upset at a slightly lower level, but it was not significant enough (5% difference) to warrant detailed investigation.

Figure 16 presents the receiver upset recovery time photographs. Extensive tests showed that the receiver determines the system recovery time. At the maximum dose rate obtainable with our test fixture (1.8×10^9 rads/s), the transmitter contributed no errors and the fiber optic cable introduced only one error (with a 100 ns recovery time). The system recovery time was in the hundreds of microseconds, so one error is insignificant. The photographs were all taken at the same dose rate (1.8×10^9 rads/s) but with varying receiver optical input power. The output is initially forced high for a period of time and then it drops low until recovery begins. The lowest input power exposure showed oscillations during recovery. The recovery time was assumed to be after the oscillations had stopped. The oscillations are visible in Figure 16(c). Since the oscilloscope time base was shorter on the first two shots, an additional shot was taken, at the optimum input levels, with the time base set to 500 μs. The same oscillation pattern was not present at the high input power levels. The recovery time is very dependent on the input power level, but it varies very little with photodiode bias.

The original plan to monitor the transmitter output with a silicon photodiode proved infeasible due to shielding problems and output amplitude problems presented by the photodiode. Therefore, the fiber optic receiver module was used to monitor the transmitter's output. This presented a problem due to the low dose rate required to upset the receiver. To determine the transmitter upset level, two separate fixtures were developed. The transmitter was mounted on one fixture encased in 5 cm lead bricks except for a 1- x 1- cm opening to the transmitter. The receiver was mounted on the other test fixture 1 m behind the transmitter and entirely encased in 5 cm lead bricks. This system worked very well, as shown by the "0" test shot in Figure 17(a). The minimum upset level proved to be 2.9×10^9 rad/s.

TOTAL NEUTRON FLUENCE TESTS

Neutron irradiations were performed with Sandia National Laboratories Pulsed Reactors (SPRII and SPRIII). All of the devices were passively irradiated and electrically evaluated as in Section I after each neutron exposure.

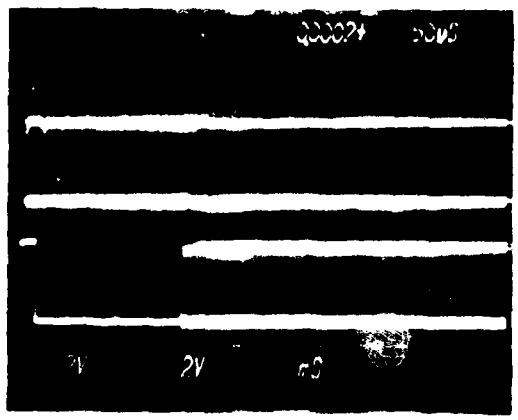

(a) Recovery time: 160μs
Optical Power: 32μW

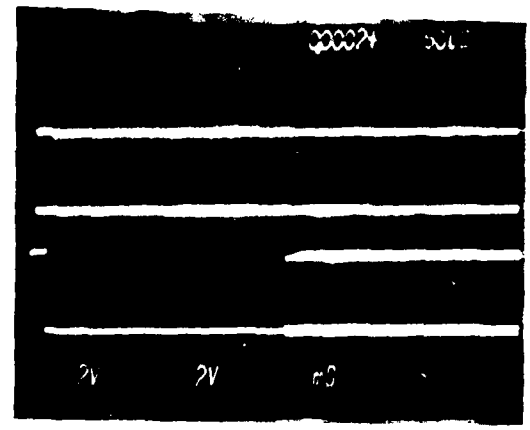

(b) Recovery time: 265μs
Optical power: 5.5μW

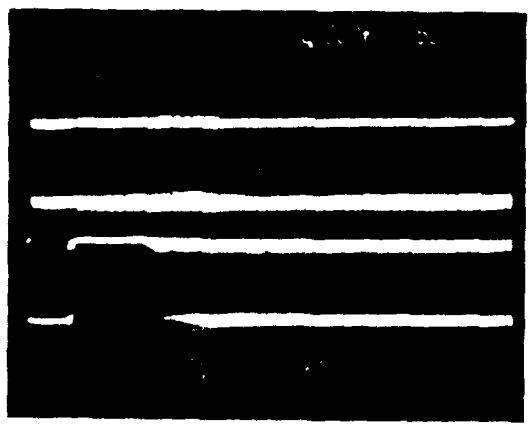

(c) Recovery time: 2.7ms
Optical power: 650nW

The top trace in all photos is the input to the transmitter, and the bottom trace is the receiver output. The pulse occurs at the beginning (.50ns) of the trace. The dose rate in all photos is 1.8×10^9 rad(Si)/s.

Figure 16. Receiver Recovery Times With Varying Optical Input Power

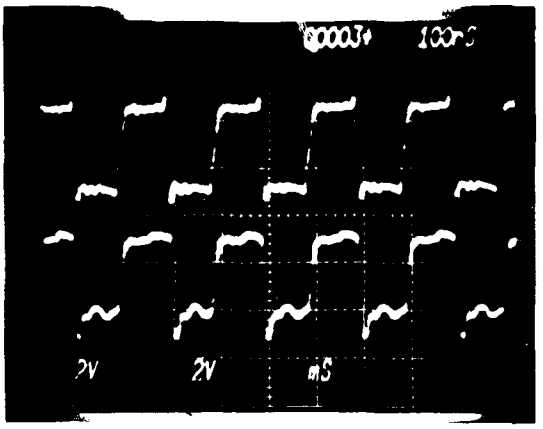

(a) "0" test, all circuit shielded.

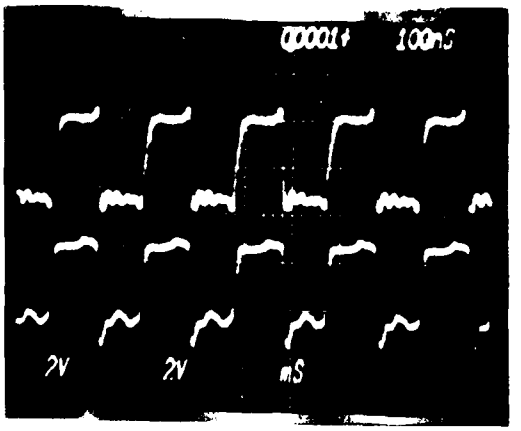

(b) 0 errors.
Dose rate: 7×10^{8} rads/s

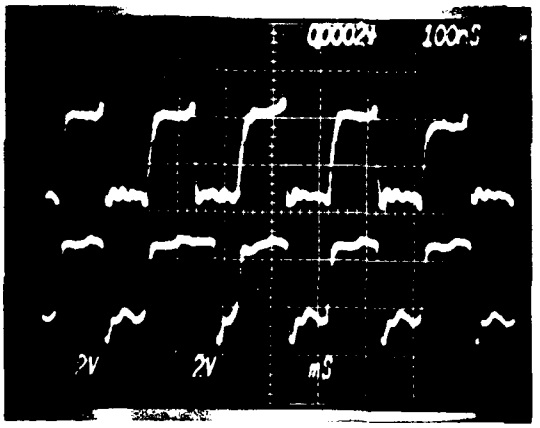

(c) 1 error.
Dose rate: 2.9×10^{9} rads/s

The top trace in all photos is the input to the transmitter, and the bottom trace is the shielded receiver's output.

Figure 17. Transmitter Minimal Upset Level

The following pages present tables of data, or graphical representations of data, for the receivers (the data tables for the graphs are in Appendix D).

Figure 18 displays the receiver minimum power for operation as following the same general pattern as appeared in the total gamma dose tests. Even with the improvement after the 8.3×10^{13} n/cm^2 irradiation, the receiver still fails to meet the manufacturer's specification of 700 nW after approximately 2×10^{13} n/cm^2 has been absorbed.

The minimum photodiode bias (Figure 19) can only be approximated below the 5.52×10^{13} n/cm^2 fluence because no data were taken before that. Initially, the minimum bias necessary was 1.45 V. The devices had always been evaluated with a photodiode bias of 5 V because that bias would allow single power supply operation if necessary. At approximately 3×10^{13} n/cm^2 this single power supply option is no longer viable. Operational problems were never observed before the 5.52×10^{13} n/cm^2 irradiation. The devices had always been slower at the 5 V bias (versus the 30 V bias) but had required 3% - 5% less light input. When the photodiode bias passed 5 V, the necessary light input was no longer dependent on the photodiode bias; but the device was still slower until the minimum bias began to approach 30 V.

The BER plot (Figure 20) is an average of the errors introduced by the two receivers. As can be seen, the BER increases rapidly as the neutron fluence approaches 10^{14} n/cm^2 and exceeds the manufacturer's specifications after the 8.3×10^{13} n/cm^2 irradiation. The BER is expressed in units of errors per pulse or bit. In the test case, the bit length was 100 ns.

The propagation delay and power supply current measurements (Tables 25 and 26) show very little change over the range of neutron fluences. Only the delay time data for a photodiode bias of 30 V is presented because the 5 V bias could not be obtained for most of the fluence levels. Since the minimum power for operation approached the 2.52 μW standard level, the delay time and power supply current measurements were done only at the minimum power for operation level because the variance was insignificant between the 2.52 μW level and the minimum power level.

The rise and fall time data tables appear in Appendix D. There was no notable change in either of these parameters throughout evaluation. At all observed neutron fluences, the rise and fall times were well within the manufacturer's specified limit.

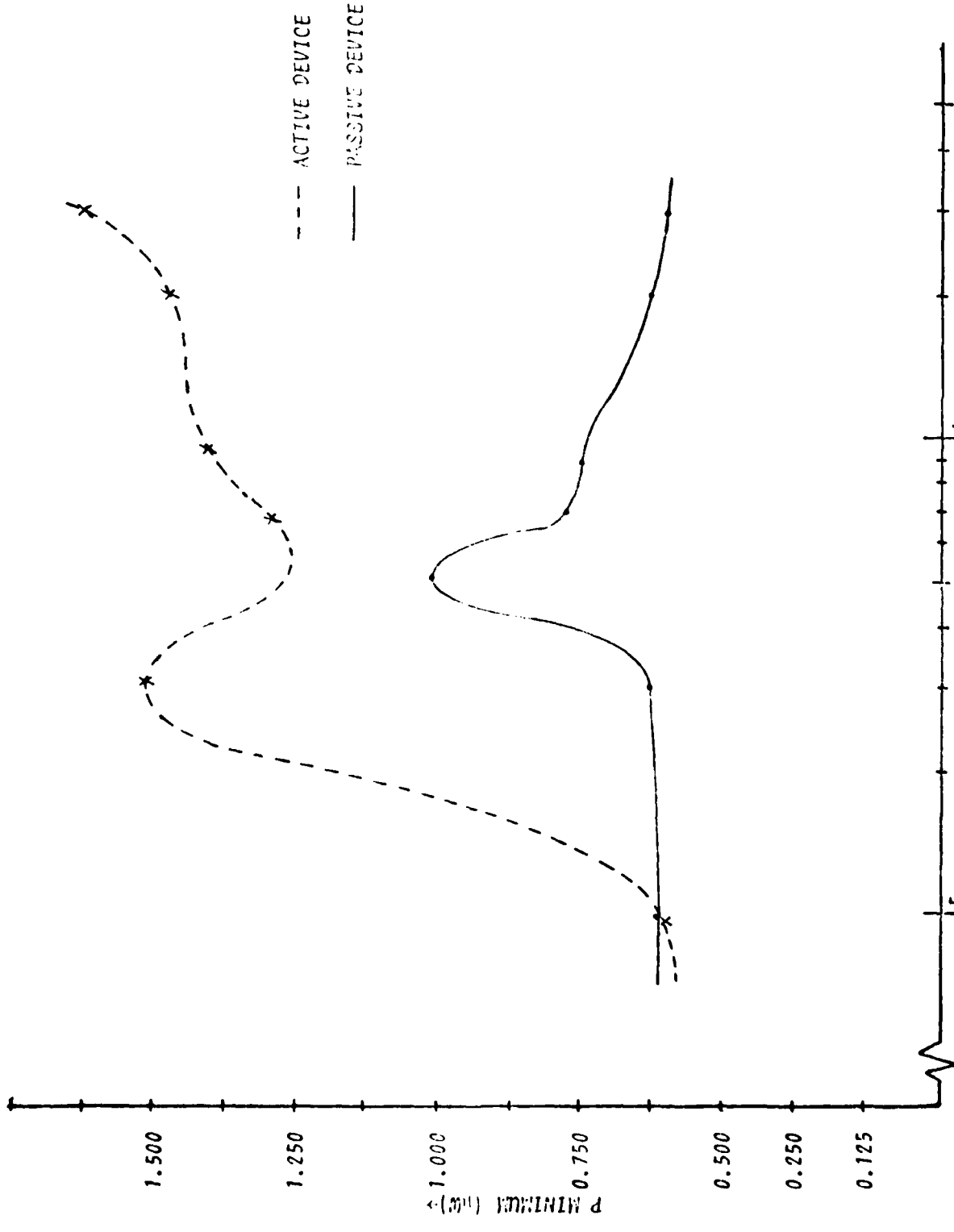

Figure 18. Receiver minimum power for operation vs. total gamma dose.

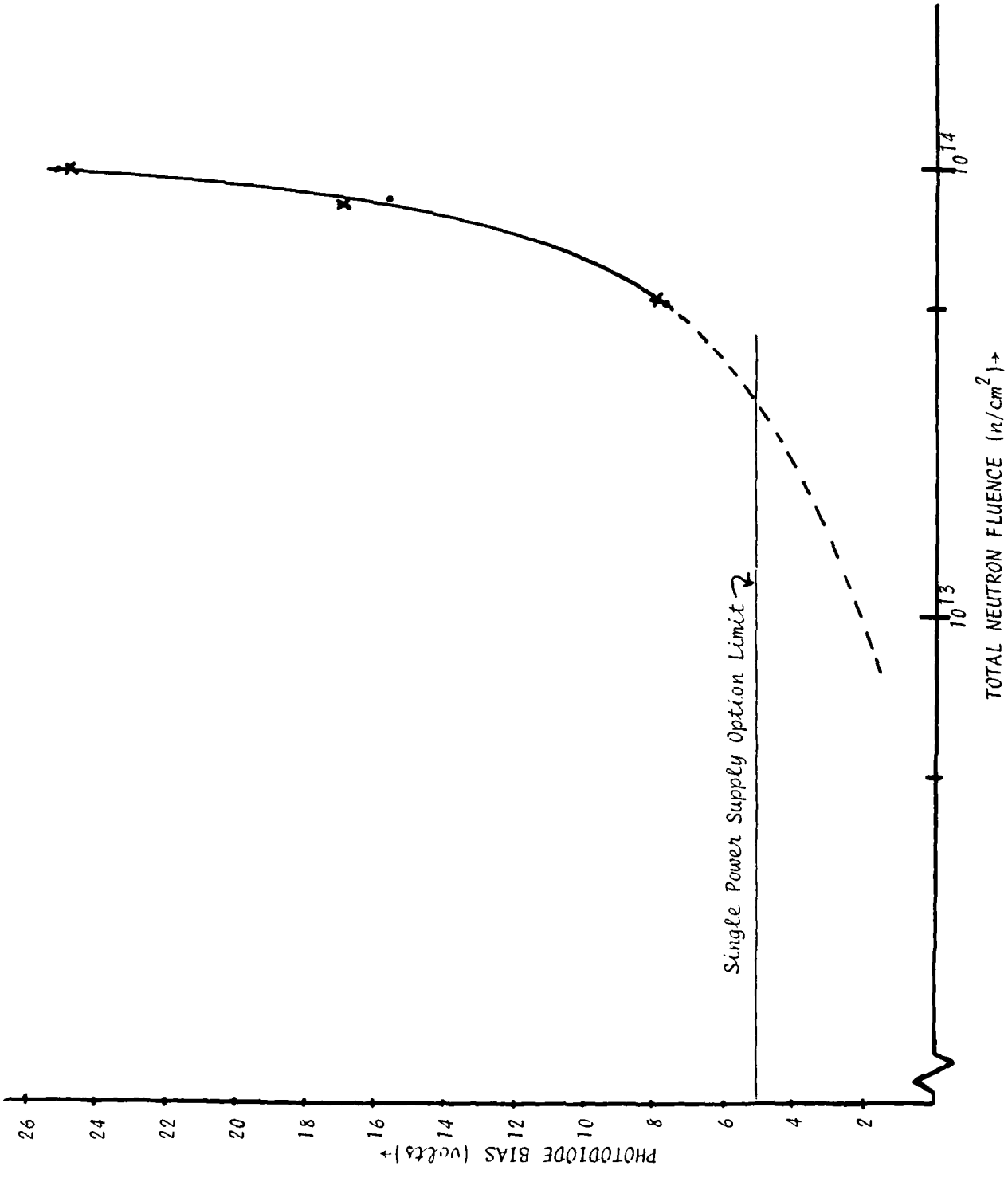

Figure 19. Minimum photodiode bias vs. total neutron fluence

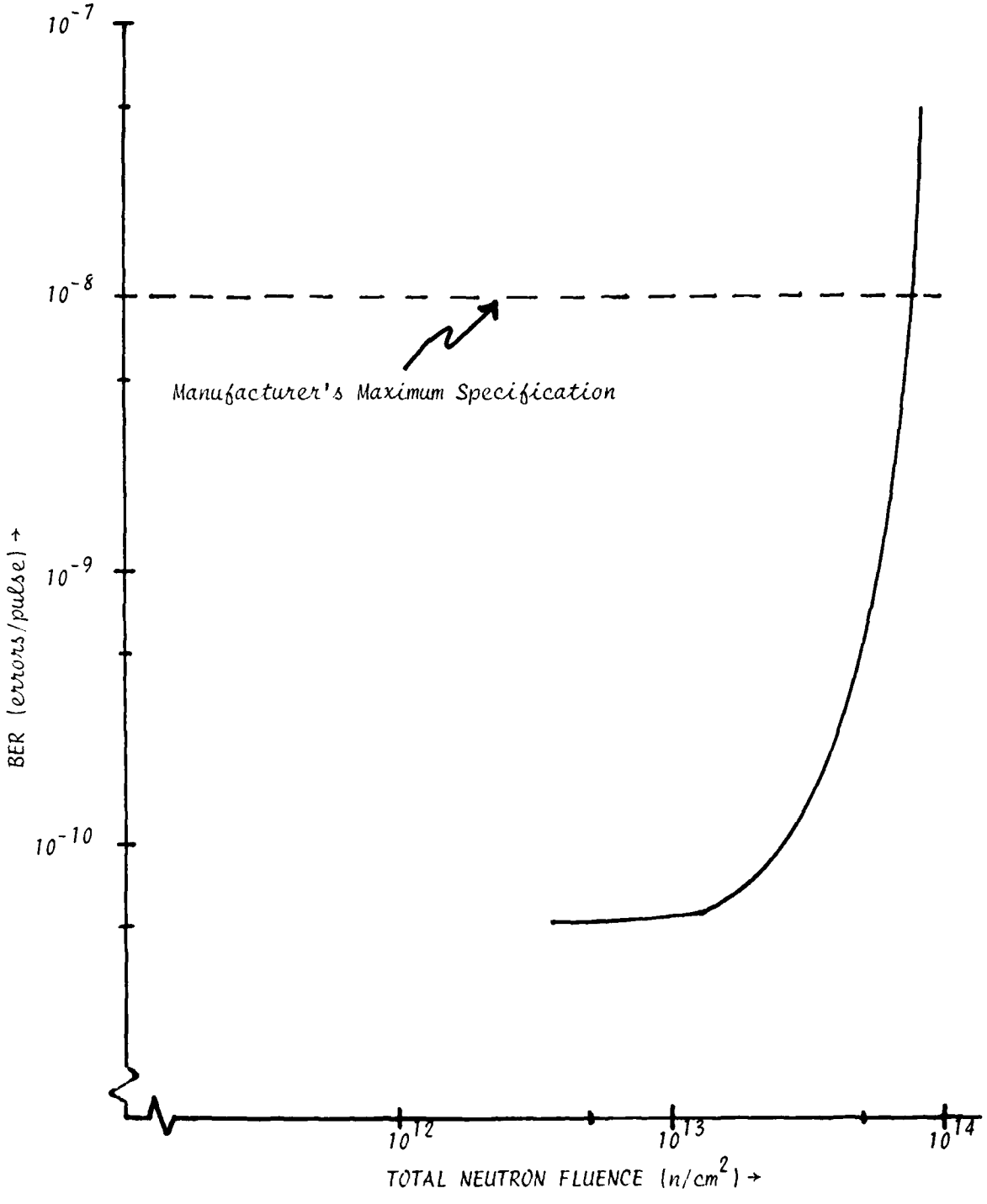

Figure 20. Bit Error Rate (BER) vs. total neutron fluence

Figure 21 and Table 27 present the transmitter's normalized optical output power and power supply current, respectively.

The two transmitters show almost exactly the same amount of degradation in optical output intensity (the normalized optical output power was computed the same as in the total dose tests). After a neutron fluence of 8.3×10^{13} n/cm^2 is reached, the optical output power of the transmitter has degraded by 90%. The power supply current shows a small reduction throughout testing (an average total of 2 mA), but this degradation does not seem to be significant enough to degrade the output by 90%.

The input current data tables are in Appendix D. There was a small, consistent decrease in all of the currents measured. The input high current measurements were performed with the input not under test at ground, so that direct comparison with the manufacturer's specifications is possible. The input high current decreased an average of 5 nA and the input low current an average of 5 μA.

TABLE 27. TRANSMITTER POWER SUPPLY CURRENT VS. TOTAL NEUTRON FLUENCE

$\Psi(n/cm^2)$	T1		T2	
	I_{CCH}(ma)	I_{CCL}(ma)	I_{CCH}(ma)	I_{CCL}(ma)
0	117.1	29.3	118.7	29.7
6.83×10^{12}	117.0	29.2	118.5	29.6
1.25×10^{13}	116.9	29.2	118.4	29.5
5.52×10^{13}	116.2	29.0	117.7	29.4
8.30×10^{13}	115.8	29.0	117.2	29.2
1.01×10^{14}	115.6	28.8	116.9	29.2

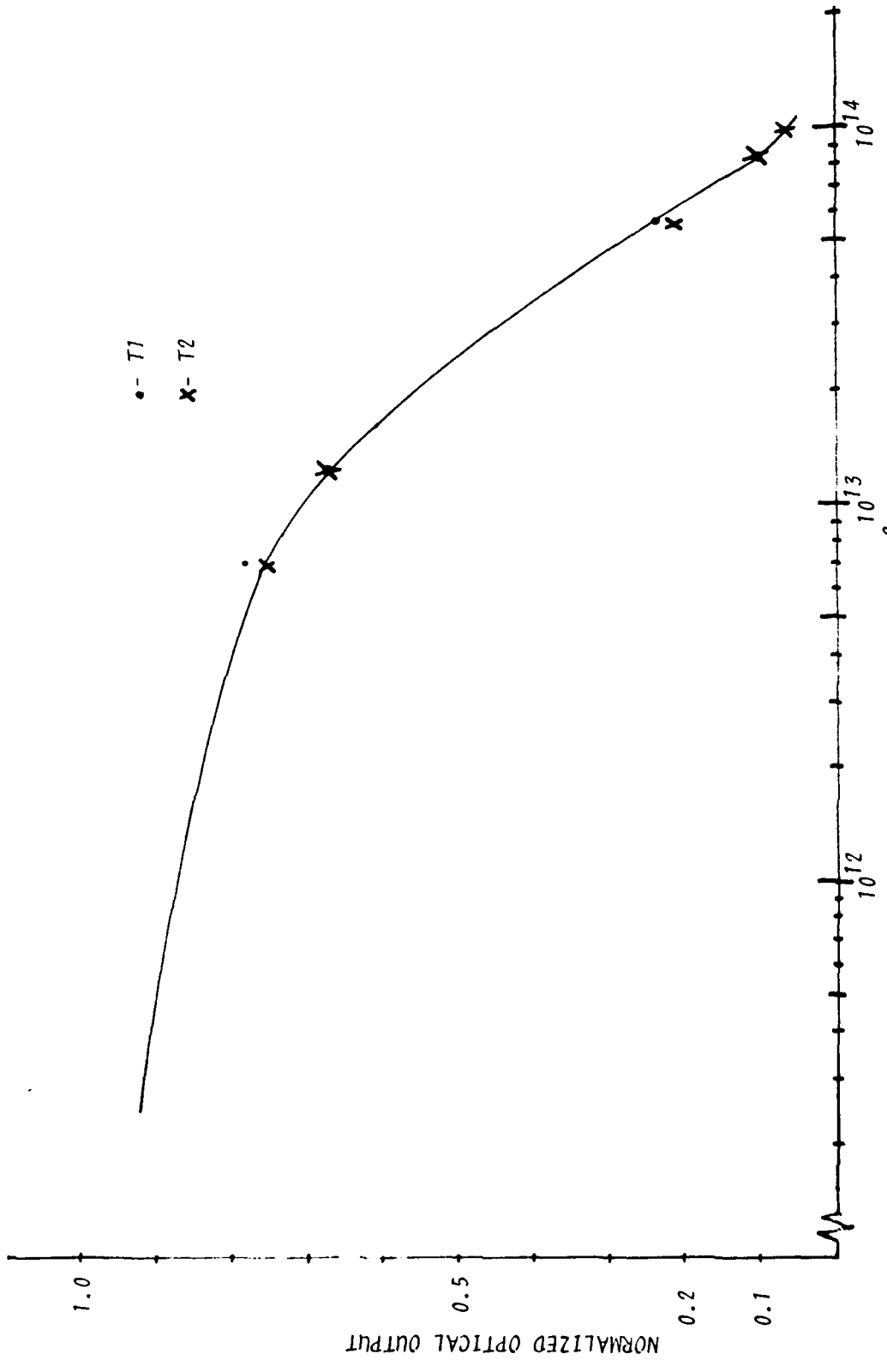

Figure 21. Transmitter normalized optical output vs. total neutron fluence.

TABLE 25. RECEIVER PROPAGATION DELAY (FOR V_B = 30 V, P = MINIMUM FOR OPERATION) VS. TOTAL NEUTRON FLUENCE

$\Psi(n/cm^2)$	R1		R2	
	$t_{D(L-H)}$ (ns)	$t_{D(L-H)}$ (ns)	$t_{D(L-H)}$ (ns)	$t_{D(L-H)}$ (ns)
0	58	56	58	60
6.83×10^{12}	57	55	58	55
1.25×10^{13}	58	55	58	55
5.52×10^{13}	53	51	52	50
8.30×10^{13}	54	51	54	50
1.01×10^{14}	56	57	56	55

TABLE 26. RECEIVER POWER SUPPLY CURRENT VS. TOTAL NEUTRON FLUENCE

$\Psi(n/cm^2)$	R1		R2	
	I_H(ma) [1]	I_M(ma) [2]	I_H(ma)	I_M(ma)
0	49.1	48.7	48.4	49.4
6.83×10^{12}	47.4	48.4	48.5	49.4
1.25×10^{13}	47.5	48.7	48.4	49.3
8.30×10^{13}	-	47.6	-	48.3
1.01×10^{14}	-	48.9	-	49.5

[a] I_H is measured when the optical input power to the receiver is 2.52 μW.

[b] I_M is measured when the optical input power to the receiver is the minimum to permit operation.

VII. CONCLUSION (SPX 4125. SPX 4126)

The transmitter module performed poorly in the total gamma dose and neutron environments when compared to the transmitter IC tested in Sections II-IV of this report. This fact is evidenced in Table 28 which is a short comparison of the two devices in different radiation environments. The module lost 28% of its optical output after absorbing 3 Mrad(Si) of the total gamma dose. It lost 93% of its optical output after a total neutron fluence of 10^{14} n/cm^2 had been reached. The minimum logic upset occurred at a dose rate of 2.9×10^9 rad(Si)/s. Figure 22 contains functional diagrams for the modules and ICs.

The receiver module and IC are compared in Table 29. Again the modules performed very poorly when compared to the ICs. A biased receiver module more than doubled its minimum power for operation after absorbing 300 krad(Si) of total gamma dose. The module experienced dose rate upsets as low as 1.3×10^6 rad(Si)/s even with all of the input parameters optimized. This level is reduced substantially with any decrease in the optical input power. Decreasing the optical input also increases the upset recovery time tremendously. In the neutron environment, the minimum photodiode bias to permit operation greatly increased. The bias exceeds 5 V after 5.5×10^{13} n/cm^2 have been absorbed, and increases to more than 25 V after the 10^{14} n/cm^2 fluence level. Up to the point that this bias level exceeds 5 V, a single power supply can be used to operate these devices. The BER of the receivers exceeds the manufacturer's specification of 10^{-8} after absorbing an 8×10^{13} n/cm^2 fluence.

The modular construction of the SPX 4125 and SPX 4126 make it difficult to determine the exact cause of the devices' degradation. From Tables 28 and 29, it is obvious that the modules are more susceptible to radiation than the ICs are. Since these modules incorporate the ICs tested and the respective diodes, it can be assumed that the critical components are the optical diodes. These diodes are the only major addition to the ICs to make up the modules. The relative hardness of the ICs compared to the modules seems to indicate that the additions would be the source of degradations. In a neutron fluence environment, degradation is caused by displacement damage. The crystal lattice is disturbed creating recombination centers. This reduces the minority carrier lifetime, thereby degrading the LED light output and current generation in the photodiode. The increases in the receiver's BER could be a combination of the

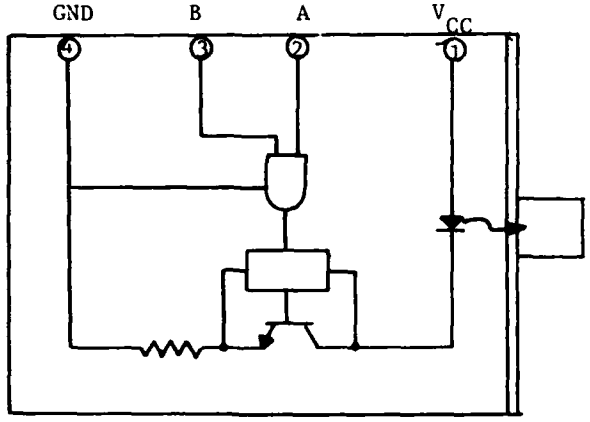

SPX4125

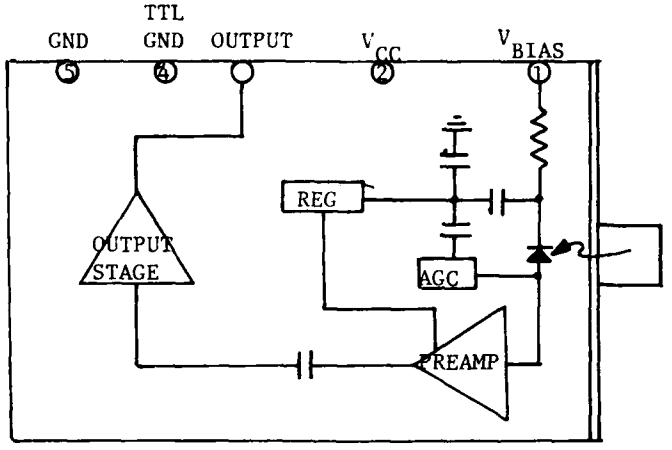

SPX4126

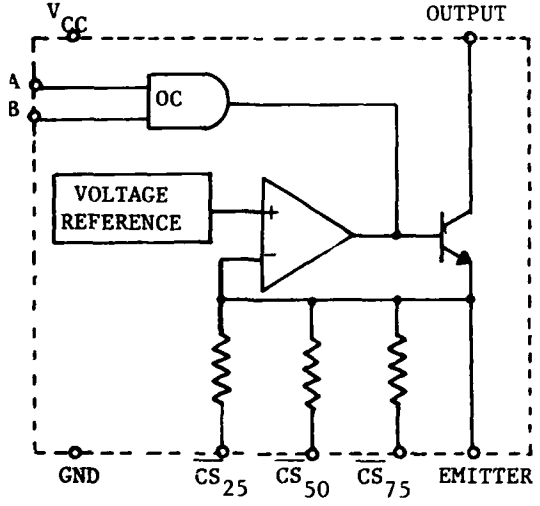

SPX3619

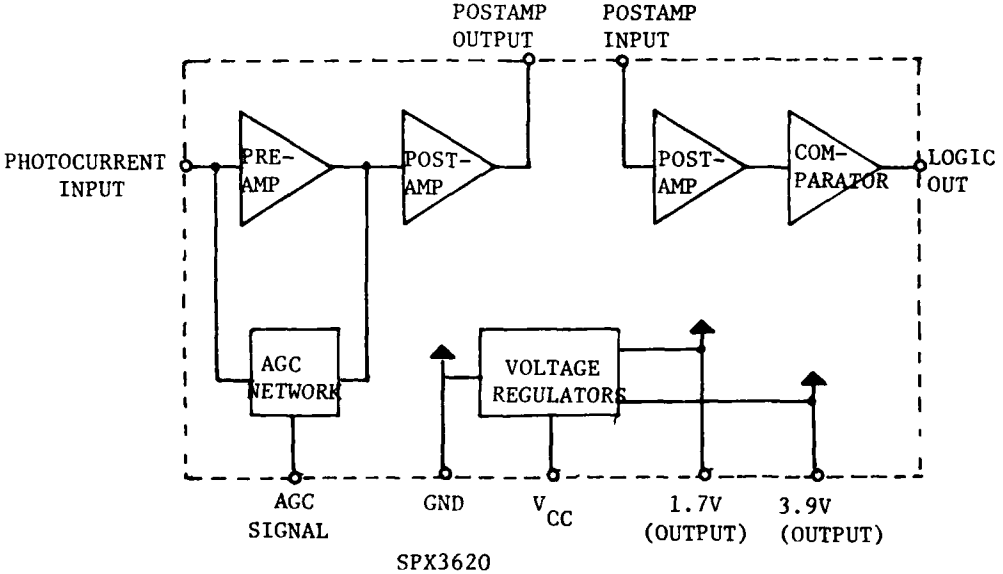

SPX3620

Figure 22. Functional diagrams of devices tested.

TABLE 28. TRANSMITTER COMPARISON IN DIFFERENT RADIATION ENVIRONMENTS

RADITION ENVIRONMENT	SPX 3619 [1]		SPX 4125 [2]	
	CHANGE IN LED DRIVE CURRENT(%)		CHANGE IN RELATIVE LIGHT OUTPUT(%)	
TOTAL GAMMA DOSE (rads(Si))	ACTIVE	PASSIVE	ACTIVE	PASSIVE
100k	-2 [3]	-1	-13	-14
500k	-2	-2	-12	-12
1M	-1	-3	-18	-- [4]
TOTAL NEUTRON FLUENCE (n/cm^2)	ALL DEVICES PASSIVELY IRRADIATED		ALL DEVICES PASSIVELY IRRADIATED	
5×10^{12}	0		-17	
1×10^{13}	0		-30	
5×10^{13}	-1		-79	
IONIZING DOSE RATE	MINIMUM UPSET LEVEL (rads(Si)/s)		MINIMUM UPSET LEVEL (rads(Si)/s)	
	1.5×10^9 LED DRIVE CURRENT=75ma		2.9×10^9	

[a]The SPX 3619 is the fiber optic transmitter IC tested.

[b]The SPX 4125 is a fiber optic module incorporating the SPX 3619 and a GaAlAs LED.

[c]A negative percentage indicates a reduction in the parameter.

[d]The passive device failed between the 500 krad(Si) and 1 Mrad(Si) exposures. This was a reliability problem and not radiation induced.

NOTE: Percent change is expressed in relation to the preradiation value.

TABLE 29. RECEIVER COMPARISON IN DIFFERENT RADIATION ENVIRONMENTS

RADIATION ENVIRONMENT	SPX 3620 [1]		SPX 4126 [2]	
	CHANGE IN MINIMUM OPERATING CURRENT(%) [3]		CHANGE IN MINIMUM OPTICAL INPUT(%)	
TOTAL GAMMA DOSE (rads(Si))	ACTIVE	PASSIVE	ACTIVE	PASSIVE
100k	+4	+3	-22 [4]	-10
500k	-2	-5	+79	+61
1M	-1	-6	+105	+12
TOTAL NEUTRON FLUENCE (n/cm^2)	ALL DEVICES PASSIVELY IRRADIATED		ALL DEVICES PASSIVELY IRRADIATED	
5×10^{12}	-1		+4	
1×10^{13}	-4		+24	
5×10^{13}	-8		+412	
IONIZING DOSE RATE	MINIMUM UPSET LEVEL (rads(Si)/s)		MINIMUM UPSET LEVEL (rads(Si)/s)	
	3.5×10^6 PHOTODIODE CURRENT=2 A		1.3×10^6 OPTICAL INPUT=32 W	

[a]The SPX 3620 is the fiber optic receiver IC tested.

[b]The SPX 4126 is a fiber optic module incorporating the APX 3620 IC and a silicon PIN photodiode.

[c]The minimum operating current is the minimum photodiode current that allows operation of the system.

[d]A negative percentage indicates a net reduction in this parameter.

NOTE: Percent change is expressed relative to the preradiation value.

photodiode degradation and amplifier degradation, but again the relatively small change in the receiver IC BER would seem to point primarily at the photodiode. In the gamma dose environment, reverse bias leakage currents are substantially increased by the introduction of surface defects. These leakage currents seriously affect the photodiodes efficiency. A forward biased junction can be affected by a charge buildup which lessens the junction field gradient.

Investigation has shown that these diodes are not typical of state-of-the-art hardened diode technologies (Refs. 1 and 2). The nuclear survivability of the modules could be greatly improved by integrating into the modules, diodes that have been tested and proven less susceptible to nuclear radiation.

An operational system composed of these modules will be limited by the receiver. Several design considerations should be noted before these modules are considered for use in a transmission link that has a nuclear survivability requirement. As a system is irradiated, the transmitter's output will decrease, the cable's transmission efficiency decreases, and the minimum power for receiver operation will increase. This combination will seriously limit the length of the fiber optic link. For example, using the fiber optic cable used in our tests (Galite TM 3000), which has a 60 dB/km loss parameter, a signal could be transmitted 430 m. After absorbing a fluence of 5.5×10^{13} n/cm^2 (and no gamma dose), this length would be reduced to 220 m. This calculation neglects any radiation damage to the fiber optic cable (which is not significant). Damage to the fiber would further sorten the link. This type of radiation degradation and the increase in the system BER should weigh heavily in system selection.

1. Barnes, C. E., Radiation Effects in Optoelectronic Devices, SAND76-0726, Sandia National Laboratories, Albuquerque, NM., March 1977.

2. Polimadei, R. A.; Share, S.; Epstein, A. S.; Lynch, R. J.; and Sullivan, D., IEE Trans. Nuc. Sci. NS-21, No. 6, 96, 1974.

APPENDIX A

SPX 3619 AND SPX 3620 NEUTRON TEST DATA

TRANSMITTER No._____	DATE: LEVEL:	5/17/79 PRE RAD	5/21/79 1.E+03	5/22/79 5.E+03	5/22/79 1.E+04	5/23/79 5.E+04	5/23/79 1.E+05	5/24/79 5.E+05	5/25/79 1.E+06	6/14/79 5.E+06
I_d - 50mA	(mA)	50.700	50.700	50.700	50.600	50.500	50.200	50.200	50.400	50.200
I_d - 75mA	(mA)	75.300	75.400	75.400	75.300	75.100	74.400	74.600	74.800	74.300
I_d - 25mA	(mA)	25.700	25.600	25.700	25.700	25.600	25.300	25.400	25.400	25.400
I_d - 150mA	(mA)	150.000	148.700	148.400	148.300	147.900	147.100	146.700	146.900	146.200
I_d - off	(μA)	2.090	1.927	1.885	1.877	1.882	1.847	1.885	1.794	1.729
I_{cc}	(mA)	32.200	32.200	32.200	32.200	32.200	32.000	31.800	31.800	31.600
I_{IL} - PIN 10	(mA)	-1.091	-1.120	-1.114	-1.111	-1.114	-1.103	-1.095	-1.083	-1.055
I_{IH} - PIN 11	(μA)	.031	.070	.035	.028	.033	.024	.073	.025	.019
I_{IL} - PIN 11	(mA)	-1.091	-1.118	-1.113	-1.110	-1.112	-1.101	-1.093	-1.079	-1.052
I_{IH} - PIN 10	(μA)	.027	.067	.034	.026	.031	.023	.065	.024	.018

TRANSMITTER No. 4	DATE: LEVEL:	5/17/79 PRE RAD	5/21/79 1.E+03	5/22/79 5.E+03	5/22/79 1.E+04	5/23/79 5.E+04	5/23/79 1.E+05	5/24/79 5.E+05	5/25/79 1.E+06	6/14/79 5.E+06
I_d - 50mA	(mA)	50.900	50.800	50.700	50.600	50.400	50.300	50.200	50.300	49.800
I_d - 75mA	(mA)	75.200	75.300	75.300	75.300	75.000	74.600	74.400	74.600	73.900
I_d - 25mA	(mA)	25.500	25.800	25.800	25.700	25.600	25.400	25.300	25.300	25.100
I_d - 150mA	(mA)	149.900	148.700	148.400	148.500	147.500	147.100	146.000	146.000	144.300
I_d - off	(μA)	2.070	1.906	1.881	1.864	1.862	1.344	1.809	1.829	1.715
I_{cc}	(mA)	32.100	32.100	32.100	32.100	32.000	31.900	31.700	31.700	31.500
I_{IL} - PIN 10	(mA)	-1.090	-1.111	-1.108	-1.108	-1.102	-1.095	-1.090	-1.080	-1.059
I_{IH} - PIN 11	(μA)	.022	.049	.032	.020	.020	.018	.019	.052	.015
I_{IL} - PIN 11	(mA)	-1.090	-1.111	-1.108	-1.107	-1.100	-1.095	-1.088	-1.079	-1.057
I_{IH} - PIN 10	(μA)	.018	.047	.031	.019	.019	.017	.018	.048	.012

TRANSMITTER No. 5	DATE: LEVEL:	5/17/79 PRE RAD	5/21/79 1.E+03	5/22/79 5.E+03	5/22/79 1.E+04	5/23/79 5.E+04	5/23/79 1.E+05	5/24/79 5.E+05	5/25/79 1.E+06	6/14/79 5.E+06
I_d - 50mA	(mA)	50.800	50.900	50.800	50.800	50.400	50.300	49.900	49.700	48.100
I_d - 75mA	(mA)	75.300	75.500	75.400	75.400	74.800	74.600	74.000	73.700	72.800
I_d - 25mA	(mA)	25.700	25.700	25.800	25.900	25.700	25.400	25.200	25.100	24.300
I_d - 150mA	(mA)	150.200	149.300	149.500	149.500	148.500	147.800	146.400	145.500	143.300
I_d - off	(μA)	1.881	1.910	1.905	1.875	1.867	1.854	1.799	1.755	1.700
I_{cc}	(mA)	32.000	32.400	32.200	32.100	32.100	31.900	31.700	31.400	31.000
I_{IL} - PIN 10	(mA)	-1.128	-1.150	-1.150	-1.148	-1.145	-1.138	-1.127	-1.120	-1.102
I_{IH} - PIN 11	(μA)	.032	.054	.056	.034	.030	.028	.036	.037	.017
I_{IL} - PIN 11	(mA)	-1.127	-1.149	-1.149	-1.147	-1.143	-1.136	-1.125	-1.118	-1.099
I_{IH} - PIN 10	(μA)	.029	.051	.052	.032	.028	.026	.032	.034	.017

TRANSMITTER No. 6	DATE:	5/17/79	5/21/79	5/22/79	5/22/79	5/23/79	5/23/79	5/24/79	5/25/79	6/14/79
	LEVEL:	PRE RAD	1.E+03	5.E+03	1.E+04	5.E+04	1.E+05	5.E+05	1.E+06	5.E+06
I_d - 50mA	(mA)	50.300	50.100	50.000	50.000	49.600	49.400	48.900	48.700	48.300
I_d - 75mA	(mA)	74.400	74.500	74.500	74.400	73.800	73.500	72.800	72.400	71.800
I_d - 25mA	(mA)	25.500	25.600	25.300	25.500	25.200	24.900	24.900	24.700	24.400
I_d - 150mA	(mA)	146.700	146.900	146.700	146.500	145.600	144.900	143.200	142.200	140.600
I_d - off	(μA)	1.831	1.847	1.884	1.831	1.817	1.803	1.747	1.765	1.607
I_{cc}	(mA)	31.600	31.400	31.400	31.300	31.000	31.000	30.800	30.500	30.200
I_{IL} - PIN 10	(mA)	-1.096	-1.097	-1.097	-1.095	-1.094	-1.088	-1.079	-1.072	-1.057
I_{IH} - PIN 11	(μA)	.037	.040	.069	.031	.026	.024	.032	.087	.015
I_{IL} - PIN 11	(mA)	-1.096	-1.095	-1.096	-1.094	-1.092	-1.086	-1.075	-1.070	-1.052
I_{IH} - PIN 10	(μA)	.031	.043	.064	.030	.025	.023	.032	.079	.015

TRANSMITTER No. 8	DATE: / LEVEL:	5/17/79 PRE RAD	5/21/79 1.E+03	5/22/79 5.E+03	5/22/79 1.E+04	5/23/79 5.E+04	5/23/79 1.E+05	5/24/79 5.E+05	5/25/79 1.E+06	6/14/79 5.E+06
I_d - 50mA	(mA)	51.100	50.700	50.500	50.600	50.500	50.200	50.300	50.300	49.900
I_d - 75mA	(mA)	75.800	75.200	75.300	75.200	75.000	74.500	74.500	74.700	74.100
I_d - 25mA	(mA)	26.000	25.900	25.800	25.800	25.800	25.500	25.500	25.500	25.500
I_d - 150mA	(mA)	149.500	148.500	148.800	148.700	148.400	147.400	147.000	147.000	146.600
I_d - off	(μA)	1.980	1.970	2.130	1.886	1.872	1.854	1.839	1.844	1.724
I_{cc}	(mA)	32.400	32.100	32.100	32.300	32.100	31.800	31.700	31.700	31.600
I_{IL} - PIN 10	(mA)	-1.100	-1.122	-1.120	-1.113	-1.116	-1.111	-1.098	-1.086	-1.061
I_{IH} - PIN 11	(μA)	.033	.033	.154	.032	.029	.022	.039	.022	.021
I_{IL} - PIN 11	(mA)	-1.098	-1.119	-1.120	-1.118	-1.114	-1.109	-1.095	-1.081	-1.057
I_{IH} - PIN 10	(μA)	.031	.032	.144	.032	.026	.021	.035	.020	.019

TRANSMITTER No. 9	DATE:	5/17/79	5/21/79	5/22/79	5/22/79	5/23/79	5/23/79	5/24/79	5/25/79	6/14/79
	LEVEL:	PRE RAD	1.E+03	5.E+03	1.E+04	5.E+04	1.E+05	5.E+05	1.E+06	5.E+06
I_d - 50mA	(mA)	51.700	51.500	51.400	51.300	51.500	51.000	51.000	51.000	50.900
I_d - 75mA	(mA)	77.100	76.700	76.600	76.600	76.400	75.900	75.900	76.000	75.800
I_d - 25mA	(mA)	26.100	26.200	26.100	26.100	26.000	25.900	25.800	25.800	25.700
I_d - 150mA	(mA)	152.400	150.900	151.300	151.300	150.800	150.100	149.700	149.300	149.000
I_d - off	(μA)	1.970	1.960	2.190	1.960	1.876	1.847	1.850	1.790	1.716
I_{cc}	(mA)	31.700	31.700	31.800	31.800	31.700	31.500	31.400	31.500	31.000
I_{IL} - PIN 10	(mA)	-1.111	-1.116	-1.118	-1.117	-1.115	-1.112	-1.096	-1.083	-1.066
I_{IH} - PIN 11	(μA)	.020	.023	.212	.032	.026	.018	.045	.018	.011
I_{IL} - PIN 11	(mA)	-1.111	-1.116	-1.117	-1.116	-1.113	-1.109	-1.093	-1.080	-1.061
I_{IH} - PIN 10	(μA)	.018	.023	.201	.025	.023	.016	.041	.015	.010

APPENDIX B

SPX 3619 AND SPX 3620 TOTAL GAMMA DOSE TEST DATA

TRANSMITTER No. 10	DATE: LEVEL:	5/30 Pre RAD	6/1 $5x10^{12}$	6/6 $1x10^{13}$	6/8 $4x10^{13}$	6/12 $7x10^{13}$	6/13 $1x10^{14}$	6/14 $4x10^{14}$	6/27 $7x10^{14}$
I_d - 50mA	(mA)	50.500	50.400	50.500	50.500	50.100	49.700	48.300	46.000
I_d - 75mA	(mA)	75.200	75.000	75.100	74.900	74.400	73.900	71.700	68.100
I_d - 25mA	(mA)	25.800	25.500	25.700	25.500	25.800	25.200	24.500	23.500
I_d - 150mA	(mA)	148.400	148.100	147.800	147.000	145.300	143.800	141.400	132.000
I_d - off	(μA)	1.878	1.943	2.270	1.947	1.802	1.777	1.687	1.609
I_{cc}	(mA)	31.500	31.500	31.500	31.300	31.200	31.000	30.400	29.000
I_{IL} - PIN 10	(mA)	1.103	-1.101	-1.104	-1.094	-1.095	-1.095	1.076	-1.037
I_{IH} - PIN 11	(μA)	.061	.150	.349	.163	.032	.022	.014	.053
I_{IL} - PIN 11	(mA)	-1.108	-1.102	-1.103	-1.101	-1.093	-1.091	-1.070	-1.028
I_{IH} - PIN 10	(μA)	.059	.143	.339	.155	.031	.020	.013	.048

TRANSMITTER No. 11	DATE: LEVEL:	5/30 Pre RAD	6/1 $5x10^{12}$	6/6 $1x10^{13}$	6/8 $4x10^{13}$	6/12 $7x10^{13}$	6/13 $1x10^{14}$	6/14 $4x10^{14}$	6/27 $7x10^{14}$
I_d - 50mA	(mA)	50.300	50.300	50.300	50.100	49.800	49.500	48.300	46.400
I_d - 75mA	(mA)	74.600	74.600	74.600	74.400	73.900	73.400	71.400	68.400
I_d - 25mA	(mA)	25.300	25.300	25.400	25.300	25.100	24.900	24.400	23.600
I_d - 150mA	(mA)	148.000	147.700	147.600	146.500	144.900	145.000	141.300	133.400
I_d - off	(μA)	1.860	1.908	2.190	1.896	1.791	1.761	1.662	1.584
I_{cc}	(mA)	32.600	32.500	32.600	32.400	32.200	32.100	31.300	30.200
I_{IL} - PIN 10	(mA)	-1.086	-1.084	-1.086	-1.082	-1.075	-1.071	-1.054	-1.018
I_{IH} - PIN 11	(μA)	.085	.152	.313	.159	.067	.053	.044	.056
I_{IL} - PIN 11	(mA)	-1.084	-1.082	-1.085	-1.079	-1.072	-1.067	-1.043	-1.010
I_{IH} - PIN 10	(μA)	.065	.133	.288	.133	.049	.036	.027	.049

TRANSMITTER No. 12	DATE: LEVEL:	5/30 Pre RAD	6/1 $5x10^{12}$	6/6 $1x10^{13}$	6/8 $4x10^{13}$	6/12 $7x10^{13}$	6/13 $1x10^{14}$	6/14 $4x10^{14}$	6/27 $7x10^{14}$
I_d - 50mA	(mA)	**51.100**	51.000	51.000	50.900	50.500	50.200	48.700	46.200
I_d - 75mA	(mA)	**75.800**	75.700	75.700	75.500	74.900	74.500	72.000	68.200
I_d - 25mA	(mA)	**25.800**	25.900	25.900	25.700	25.500	25.400	24.600	23.600
I_d - 150mA	(mA)	**149.400**	149.400	149.100	148.000	146.200	145.600	142.100	132.300
I_d - off	(μA)	**1.874**	1.872	2.160	1.937	1.835	1.794	1.689	1.600
I_{cc}	(mA)	**31.500**	32.200	31.700	31.600	31.600	31.300	30.500	29.100
I_{IL} - PIN 10	(mA)	**-1.098**	-1.095	-1.099	-1.093	-1.087	-1.084	-1.065	-1.027
I_{IH} - PIN 11	(μA)	**.038**	.048	.214	.037	.035	.019	.013	.030
I_{IL} - PIN 11	(mA)	**-1.096**	-1.094	-1.098	-1.092	-1.088	-1.081	-1.059	-1.017
I_{IH} - PIN 10	(μA)	**.036**	.046	.204	.092	.032	.018	.012	.027

TRANSMITTER No. 13	DATE: LEVEL:	5/30 Pre RAD	6/1 $5x10^{12}$	6/6 $1x10^{13}$	6/8 $4x10^{13}$	6/12 $7x10^{13}$	6/13 $1x10^{14}$	6/14 $4x10^{14}$	6/27 $7x10^{14}$
I_d - 50mA	(mA)	50.500	50.400	50.400	50.400	50.000	49.600	48.100	46.500
I_d - 75mA	(mA)	75.000	75.100	74.700	74.800	74.300	73.800	71.400	68.300
I_d - 25mA	(mA)	25.000	25.400	25.600	25.400	25.200	25.000	24.300	23.500
I_d - 150mA	(mA)	147.400	147.600	147.400	146.100	144.800	143.900	140.700	132.400
I_d - off	(μA)	1.896	1.870	2.147	1.933	1.845	1.817	1.741	1.663
I_{cc}	(mA)	32.100	32.000	31.900	31.800	31.600	31.600	30.600	29.500
I_{IL} - PIN 10	(mA)	-1.115	-1.117	-1.113	-1.114	-1.110	-1.104	-1.067	-1.046
I_{IH} - PIN 11	(μA)	.038	.047	.171	.079	.031	.019	.011	.026
I_{IL} - PIN 11	(mA)	-1.115	-1.115	-1.117	-1.112	-1.107	-1.102	-1.082	-1.038
I_{IH} - PIN 10	(μA)	.034	.045	.163	.076	.028	.018	.011	.024

TRANSMITTER No. 14	DATE: LEVEL:	5/30 Pre RAD	6/1 $5x10^{12}$	6/6 $1x10^{13}$	6/9 $4x10^{13}$	6/12 $7x10^{13}$	6/13 $1x10^{14}$	6/14 $4x10^{14}$	6/27 $7x10^{14}$
I_d - 50mA	(mA)	49.100	49.000	49.000	48.900	48.600	48.300	47.000	45.200
I_d - 75mA	(mA)	73.100	73.000	73.000	72.800	72.400	71.900	69.800	66.600
I_d - 25mA	(mA)	24.800	24.700	24.700	24.600	24.500	24.400	23.800	22.900
I_d - 150mA	(mA)	144.600	144.500	144.000	143.400	141.800	140.100	137.900	123.700
I_d - off	(μA)	1.915	1.920	2.160	2.030	1.880	1.834	1.735	1.646
I_{cc}	(mA)	32.900	32.900	32.800	32.900	32.500	32.300	31.500	30.300
I_{IL} - PIN 10	(mA)	-1.150	-1.149	-1.151	-1.142	-1.140	-1.137	-1.118	-1.076
I_{IH} - PIN 11	(μA)	.033	.048	.136	.063	.027	.017	.012	.020
I_{IL} - PIN 11	(mA)	-1.149	-1.147	-1.150	-1.141	-1.138	-1.134	-1.113	-1.068
I_{IH} - PIN 10	(μA)	.031	.049	.123	.063	.027	.017	.010	.021

TRANSMITTER No. 15	DATE: LEVEL:	5/30 Pre RAD	6/1 $5x10^{12}$	6/6 $1x10^{13}$	6/8 $4x10^{13}$	6/12 $7x10^{13}$	6/13 $1x10^{14}$	6/14 $4x10^{14}$	6/27 $7x10^{14}$
I_d - 50mA	(mA)	49.600	49.500	49.500	49.400	49.100	48.800	47.500	45.700
I_d - 75mA	(mA)	73.600	73.500	73.500	73.300	72.900	72.500	70.400	67.300
I_d - 25mA	(mA)	24.900	24.900	24.900	24.800	24.700	24.600	24.000	23.200
I_d - 150mA	(mA)	146.000	145.900	145.500	144.600	143.000	143.400	139.100	131.500
I_d - off	(μA)	.192	.257	.280	215	.190	.183	.186	.210
I_{cc}	(mA)	32.600	32.600	32.700	32.500	32.500	32.100	31.500	30.400
I_{IL} - PIN 10	(mA)	-1.140	-1.142	-1.138	-1.132	-1.129	-1.128	-1.110	-1.070
I_{IH} - PIN 11	(μA)	.030	.091	.109	.052	.026	.015	.011	.021
I_{IL} - PIN 11	(mA)	-1.139	-1.140	-1.137	-1.130	-1.127	-1.125	-1.104	-1.061
I_{IH} - PIN 10	(μA)	.027	.088	.104	.049	.025	.016	.008	.020

TRANSMITTER No. 6	DATE: LEVEL:	5/30 Pre RAD	6/1 $5x10^{12}$	6/6 $1x10^{13}$	6/8 $4x10^{13}$	6/12 $7x10^{13}$	6/13 $1x10^{14}$	6/14 $4x10^{14}$	6/27 $7x10^{14}$
I_d - 50mA	(mA)	50.600	50.500	50.400	50.300	50.000	49.800	48.500	46.300
I_d - 75mA	(mA)	75.300	75.200	74.400	73.900	74.400	73.900	71.800	68.300
I_d - 25mA	(mA)	25.600	25.700	25.600	25.600	25.400	25.200	24.600	23.600
I_d - 150mA	(mA)	143.400	143.700	143.200	142.600	141.500	143.800	139.400	132.400
I_d - off	(μA)	1.841	1.856	1.883	1.825	1.789	1.775	1.656	1.545
I_{cc}	(mA)	31.400	31.400	31.400	31.200	31.100	31.000	30.100	28.900
I_{IL} - PIN 10	(mA)	-1.100	-1.099	-1.094	-1.097	-1.094	-1.081	-1.069	-1.029
I_{IH} - PIN 11	(μA)	.031	.057	.090	.044	.026	.021	.012	.018
I_{IL} - PIN 11	(mA)	1.099	1.098	-1.094	-1.095	-1.090	-1.081	-1.064	-1.020
I_{IH} - PIN 10	(μA)	.029	.054	.087	.044	.024	.019	.010	.018

TRANSMITTER S/N: _____	DATE: LEVEL:	5/30 Pre RAD	6/1 $5x10^{12}$	6/6 $1x10^{13}$	6/8 $4x10^{13}$	6/12 $7x10^{13}$	6/13 $1x10^{14}$	6/14 $4x10^{14}$	6/27 $7x10^{14}$
I_d - 50mA	(mA)	50.000	50.000	50.000	49.800	49.500	48.100	47.800	45.800
I_d - 75mA	(mA)	74.300	74.200	74.200	73.900	73.600	73.000	70.700	67.400
I_d - 25mA	(mA)	25.300	25.300	25.200	25.100	25.000	24.800	24.100	23.200
I_d - 150mA	(mA)	146.800	146.800	146.500	145.400	144.000	142.700	139.400	130.900
I_d - off	(μA)	1.861	1.896	1.890	1.895	1.892	1.784	1.681	1.581
I_{cc}	(mA)	31.700	13.600	31.500	31.600	31.200	31.200	30.200	29.000
I_{IL} - PIN 10	(mA)	-1.117	-1.116	-1.119	-1.111	-1.116	-1.102	-1.085	-1.048
I_{IH} - PIN 11	(μA)	.035	.085	.076	.044	.037	.023	.016	.022
I_{IL} - PIN 11	(mA)	-1.119	-1.119	-1.112	-1.114	-1.116	-1.103	-1.082	-1.040
I_{IH} - PIN 10	(μA)	3.320	3.360	3.420	3.340	3.200	3.020	3.010	2.950

TRANSMITTER No. 18	DATE: LEVEL:	5/30 Pre RAD	6/1 $5x10^{12}$	6/6 $1x10^{13}$	6/8 $4x10^{13}$	6/12 $7x10^{13}$	6/13 $1x10^{14}$	6/14 $4x10^{14}$	6/27 $7x10^{14}$
I_d - 50mA	(mA)	50.900	50.900	50.600	50.600	50.400	50.100	48.700	46.400
I_d - 75mA	(mA)	75.400	75.400	75.000	74.800	74.900	74.400	72.200	68.600
I_d - 25mA	(mA)	25.900	25.900	25.800	25.600	25.200	25.300	24.600	23.600
I_d - 150mA	(mA)	148.600	148.800	147.700	147.700	145.700	144.200	142.500	133.300
I_d - off	(μA)	5.350	5.410	5.440	5.370	5.430	5.500	5.390	5.110
I_{cc}	(mA)	31.500	31.600	31.600	31.500	31.200	31.100	30.300	29.000
I_{IL} - PIN 10	(mA)	-1.083	-1.081	-1.078	-1.079	-1.073	-1.070	-1.052	-1.011
I_{IH} - PIN 11	(μA)	.031	.068	.061	.045	.028	.022	.015	.020
I_{IL} - PIN 11	(mA)	-1.081	-1.080	-1.079	-1.077	-1.072	-1.066	-1.047	-1.003
I_{IH} - PIN 10	(μA)	.023	.065	.057	.042	.027	.020	.013	.018

TRANSMITTER No. 20	DATE: / LEVEL:	5/30 Pre RAD	6/1 $5x10^{12}$	6/6 $1x10^{13}$	6/8 $4x10^{13}$	6/12 $7x10^{13}$	6/13 $1x10^{14}$	6/14 $4x10^{14}$	6/27 $7x10^{14}$
I_d - 50mA	(mA)	51.200	51.100	51.100	50.900	50.600	50.300	49.000	46.800
I_d - 75mA	(mA)	76.200	76.100	76.100	75.900	75.400	74.900	72.800	69.300
I_d - 25mA	(mA)	26.100	26.000	25.900	25.800	25.700	25.600	24.900	23.300
I_d - 150mA	(mA)	150.000	150.000	149.500	148.600	146.300	145.900	143.000	134.400
I_d - off	(μA)	4.100	4.120	4.080	4.360	4.150	4.070	3.880	3.900
I_{cc}	(mA)	31.600	31.600	31.700	31.500	31.300	31.300	30.500	29.300
I_{IL} - PIN 10	(mA)	-1.100	-1.096	-1.101	-1.093	-1.092	-1.087	-1.069	-1.028
I_{IH} - PIN 11	(μA)	.034	.055	.069	.269	.029	.024	.018	.019
I_{IL} - PIN 11	(mA)	-1.098	-1.096	-1.098	-1.098	-1.090	-1.084	-1.064	-1.020
I_{IH} - PIN 10	(μA)	.034	.054	.069	.247	.031	.024	.016	.019

APPENDIX C

SPX 4125 AND SPX 4126 TOTAL GAMMA DOSE DATA TABLES

TABLE C1. RECEIVER PROPAGATION DELAY (P = 2.52 μW, V_B = 30 V) VS. TOTAL GAMMA DOSE

γ_D(rads(Si))	PASSIVE		ACTIVE	
	$t_{D(L-H)}$ (ns)	$t_{D(H-L)}$ (ns)	$t_{D(L-H)}$ (ns)	$t_{D(H-L)}$ (ns)
0	51	52	51	56
50 K	53	52	56	56
100 K	52	51	53	55
300 K	47	59	51	61
500 K	47	61	47	61
700 K	45	60	48	62
1 M	45	62	49	63
2 M	49	59	50	61
3 M	54	52	54	56

TABLE C2. RECEIVER PROPAGATION DELAY (P = P_{MIN}, V_B = 30 V) VS. TOTAL GAMMA DOSE

γ_D(rads(Si))	PASSIVE		ACTIVE	
	$t_{D(L-H)}$ (ns)	$t_{D(H-L)}$ (ns)	$t_{D(L-H)}$ (ns)	$t_{D(H-L)}$ (ns)
0	56	55	59	57
50 K	56	54	60	57.5
100 K	57	55	62	57
300 K	54	64	52	65
500 K	52	66	55	71
700 K	52	65	52	71
1 M	53	65	54	70
2 M	55	66	56	67
3 M	60	58	62	59

TABLE C3. RECEIVER RISE TIME (V_B = 5 V) VS. TOTAL GAMMA DOSE

γ_D(rads(Si))	PASSIVE		ACTIVE	
	t_{rH}(ns)	t_{rL}(ns)	t_{rH}(ns)	t_{rL}(ns)
0	6	6	11.5	11
50 K	6	6	11	11
100 K	7	8	13	12
300 K	6.5	10	13.5	15
500 K	6.5	9	11	14
700 K	5	10	11	14
1 M	6	10	11	14
2 M	7	9	12	16
3 M	8	9	11.5	11

TABLE C4. RECEIVER FALL TIME (V_B = 5 V) VS. TOTAL GAMMA DOSE

γ_D(rads(Si))	PASSIVE		ACTIVE	
	t_{fH}(ns)	t_{fL}(ns)	t_{fH}(ns)	t_{fL}(ns)
0	3	2.5	3	3
50 K	3	3	3	2
100 K	3	3	3	3
300 K	3	3	3.5	3
500 K	3	3	3	3
700 K	3	3	3	3
1 M	3	3	3	3
2 M	4	4	3.5	4
3 M	4	4	3.5	3.5

TABLE C5. RECEIVER FALL TIME (V_B = 30 V) VS. TOTAL GAMMA DOSE

γ_D(rads(Si))	PASSIVE		ACTIVE	
	t_{fH}(ns)	t_{fL}(ns)	t_{fH}(ns)	t_{fL}(ns)
0	2.5	2.5	2.5	3
50 K	2.5	3	2	2.5
100 K	2.5	3	2	2.5
300 K	3	3	3	3
500 K	3	3	3	3
700 K	3	3	3	3
1 M	3	3	3	3
2 M	4	4	3.5	4
3 M	3.5	3.5	4	3.5

TABLE C6. TRANSMITTER INPUT B CURRENT VS. TOTAL GAMMA DOSE

γ_D(rads(Si))	PASSIVE		ACTIVE	
	I_{IH} (na)	I_{IL} (ma)	I_{IH}(na)	I_{IL} (ma)
0	10	-0.988	13	-0.958
50 K	10	-0.982	14	-0.948
100 K	7	-0.982	8	-0.952
300 K	7	-0.965	10	-0.926
500 K	5	-0.963	7	-0.926
700 K	--	--	7	-0.895
1 M	--	--	7	-0.912
2 M	--	--	6	-0.907
3 M	--	--	6	-0.898

APPENDIX D

SPX 4125 AND SPX 4126 TOTAL NEUTRON FLUENCE DATA TABLES

TABLE D1. RECEIVER MINIMUM POWER FOR OPERATION VS. TOTAL NEUTRON FLUENCE

Ψ (n/cm^2)	P_{m1} (μW)	P_{m2} (μW)
0	0.626	0.480
6.83×10^{12}	0.658	0.488
1.25×10^{13}	0.771	0.594
5.52×10^{13}	2.52	2.50
8.30×10^{13}	1.14	1.09
1.01×10^{14}	1.25	1.21

TABLE D2. RECEIVER RISE TIME VS. TOTAL NEUTRON FLUENCE

Ψ(n/cm^2)	t_{r1} (ns)	t_{r2} (ns)
0	6	6
6.83×10^{12}	5	6
1.25×10^{13}	7	7
5.52×10^{13}	6	6
8.30×10^{13}	6	6
1.01×10^{14}	8	9

NOTE: Due to the minimum photodiode bias exceeding 5 V and the minimum input power approaching 2.52 μW, only data at V_B = 30 V, P = Pm were taken. This is also true for the fall time data following.

TABLE D3. RECEIVER FALL TIME VS. TOTAL NEUTRON FLUENCE

$\Psi(n/cm^2)$	t_{f1} (ns)	t_{f2} (ns)
0	2.5	2.5
6.83×10^{12}	3	3
1.25×10^{13}	3	3
5.52×10^{13}	3	3
8.30×10^{13}	3	3
1.01×10^{14}	3	3

TABLE D4. RECEIVER MINIMUM PHOTODIODE BIAS FOR OPERATION VS. TOTAL NEUTRON FLUENCE

$\Psi(n/cm^2)$	V_{B1} (v)	V_{B2} (v)
0	1.45	1.47
6.83×10^{12}	--	--
1.25×10^{13}	--	--
5.52×10^{13}	8.0	8.3
8.30×10^{13}	13.9	15.2
1.01×10^{14}	25.8	25.6

TABLE D5. TRANSMITTER NORMALIZED OPTICAL OUTPUT VS. TOTAL NEUTRON FLUENCE

$\Psi(n/cm^2)$	Φ_1	Φ_2
0	1.00	1.00
6.83×10^{12}	0.77	0.74
1.25×10^{13}	0.67	0.67
5.52×10^{13}	0.24	0.21
8.30×10^{13}	0.10	0.10
1.01×10^{14}	0.08	0.07

TABLE D6. TRANSMITTER INPUT CURRENT (T1) VS. TOTAL NEUTRON FLUENCE

$\Psi(n/cm^2)$	I_{IHA} (na)	I_{ILA}(ma)	I_{IHB}(na)	I_{ILB}(ma)
0	28	-0.981	26	-0.984
6.83×10^{12}	28	-0.979	26	-0.982
1.25×10^{13}	25	-0.983	22	-0.985
5.52×10^{13}	23	-0.978	20	-0.982
8.30×10^{13}	21	-0.976	19	-0.980
1.01×10^{14}	20	-0.977	17	-0.981

TABLE D7. TRANSMITTER INPUT CURRENT (T2) VS. TOTAL NEUTRON FLUENCE

$\Psi(n/cm^2)$	I_{IHA} (na)	I_{ILA}(ma)	I_{IHB}(na)	I_{ILB}(ma)
0	11	-0.977	28	-0.983
6.83×10^{12}	8	-0.982	26	-0.983
1.25×10^{13}	7	-0.984	22	-0.986
5.52×10^{13}	6	-0.979	23	-0.981
8.30×10^{13}	6	-0.978	23	-0.981
1.01×10^{14}	5	-0.979	20	-0.983

NOTE: Due to the minimum photodiode bias exceeding 5 V and the minimum input power approaching 2.52 μW, only data at V_B = 30 V, P = Pm were taken. This is also true for the fall time data following.

DISTRIBUTION LIST

DEPARTMENT OF DEFENSE

Defense Mat Spec & Standard Office
ATTN: L. Fox

Defense Nuclear Agency
ATTN: RAEV, M. Kemp
ATTN: RAEV, A. Kubo
ATTN: RAEV, W. Mohr
ATTN: DDST
4 cy ATTN: TITL

Defense Technical Info Center
12 cy ATTN: DD

Field Command
Defense Nuclear Agency
ATTN: FCPR

Field Command
Defense Nuclear Agency
Livermore Division
ATTN: FCPRL

National Security Agency
ATTN: G. Daily
ATTN: T. Brown
ATTN: P. Deboy

Undersecretary of Def for Rsch & Engrg
ATTN: Strategic & Space Systems (OS)

Command & Control Technical Center
Department of Defense
ATTN: C-362, G. Adkins

Defense Advanced Rsch Proj Agency
ATTN: J. Fraser
ATTN: R. Reynolds

Defense Electronic Supply Center
ATTN: DEFC-ESA

DEPARTMENT OF THE ARMY

BMD Advanced Technology Center
Department of the Army
ATTN: ATC-T
ATTN: ATC-O, F. Hoke

BMD Systems Command
Department of the Army
ATTN: BMDSC-HW, R. Dekalb

Deputy Chief of Staff for Rsch Dev & Acq
Department of the Army
ATTN: M. Gale

Harry Diamond Laboratories
Department of the Army
ATTN: DELHD-N-RBH, J. Halpin
ATTN: DELHD-N-RBH, H. Eisen
ATTN: DELHD-N-P
ATTN: DELHD-N-RBH
ATTN: DELHD-N-RBC, J. McGarrity
ATTN: DELHD-N-P, F. Balicki

DEPARTMENT OF THE ARMY (Continued)

U.S. Army Armament Research & Dev Command
ATTN: DRDAR-LCA-PD

U.S. Army Communications R&D Command
ATTN: D. Huewe
ATTN: AMSEL-VL-A, Parent
ATTN: ORSEL-CT-L, Buser
ATTN: AMSEL-TL-M, Tenzer

U.S. Army Material & Mechanics Rsch Ctr
ATTN: DRXMR-H, J. Hofmann

U.S. Army Nuclear & Chemical Agency
ATTN: Library

DEPARTMENT OF THE NAVY

Naval Electronic Systems Command
ATTN: Code 5045.11, C. Suman

Naval Ocean Systems Center
ATTN: Code 4471, Tech Library

Naval Research Laboratory
ATTN: Code 6816, D. Patterson
ATTN: Code 6810, J. Davey
ATTN: Code 6813, J. Killiany
ATTN: Code 4701, J. Brown
ATTN: Code 6650, A. Namenson
ATTN: Code 6600, J. McEllinney
ATTN: Code 6601, E. Wolicki
ATTN: Code 6627, C. Guenzer
ATTN: Code 6816, H. Hughes

Naval Sea Systems Command
ATTN: SEA-06J, R. Lane

Naval Surface Weapons Center
ATTN: Code F31
ATTN: Code F30

Naval Weapons Center
ATTN: Code 233, Tech Library

Naval Weapons Evaluation Facility
ATTN: Code AT-6

Naval Weapons Support Center
ATTN: Code 70242, J. Munarin
ATTN: Code 7024, J. Ramsey
ATTN: Code 7024, T. Ellis

Office of Naval Research
ATTN: Code 220, D. Lewis
ATTN: Code 427, L. Cooper
ATTN: Code 411, Hodkins

Strategic Systems Project Office
Department of the Navy
ATTN: NSP-230, D. Gold
ATTN: NSP-27331, P. Spector
ATTN: NSP-2701, J. Pitsenberger
ATTN: NSP-2015

DEPARTMENT OF THE AIR FORCE

Air Force Aero-Propulsion Lab
ATTN: POD, P. Stover

Air Force Geophysics Lab
ATTN: SULL
ATTN: SULL S-29

Air Force Institute of Technology
ATTN: ENP, J. Bridgeman

Air Force Materials Lab
ATTN: LPO, R. Hickmott
ATTN: LTE

Headquarters
Air Force Systems Command
ATTN: DLW
ATTN: DLCA
ATTN: DLCAM, T. Seale
ATTN: XRLA, R. Stead
ATTN: IN

Air Force Technical Applications Ctr
ATTN: TAE

Air Force Weapons Lab
Air Force Systems Command
ATTN: NTYCT, J. Ferry
ATTN: NTMD, G. Chapman
ATTN: NTYCT, J. Mullis
ATTN: NTYCT, R. Maier
3 cy ATTN: SUL
5 cy ATTN: NTYCT, K. Loree

Air Force Wright Aeronautical Labs
ATTN: TEA, R. Conklin
2 cy ATTN: AADE-3, M. St Jonn

Air Logistics Command
Department of the Air Force
ATTN: OO-ALC/MM, R. Blackburn
ATTN: MMEDD
ATTN: MMETR

Ballistic Missile Office
Air Force Systems Command
ATTN: MNNL
ATTN: MNRTE
ATTN: MNNG
ATTN: MNNH, J. Tucker

Foreign Technology Division
Air Force Systems Command
ATTN: TQTD, B. Ballard
ATTN: PDJV

Headquarters Space Division
Air Force Systems Command
ATTN: C. Kelly

Headquarters Space Division
Air Force Systems Command
ATTN: AQT, W. Blakney
ATTN: AQM

Headquarters Space Division
Air Force Systems Command
ATTN: SZJ, R. Davis

DEPARTMENT OF THE AIR FORCE (Continued)

Rome Air Development Center
Air Force Systems Command
ATTN: RBCT, R. Stratton
ATTN: RBRM, T. Dellecove
ATTN: ESO, Yang
ATTN: DCLT, Levi

Rome Air Development Center
Air Force Systems Command
ATTN: ETS, R. Dolan
ATTN: ESE, A. Kahan
ATTN: ESR, W. Shedd
ATTN: ESER, R. Buchanan
ATTN: ESR, P. Vail

Strategic Air Command
Department of the Air Force
ATTN: XPFS, M. Carra

USAF/SAMID
ATTN: SAMID

DEPARTMENT OF ENERGY

Department of Energy
ATTN: WSSB

DEPARTMENT OF ENERGY CONTRACTORS

Lawrence Livermore National Lab
ATTN: Technical Info Dept

Los Alamos Scientific National Lab
ATTN: J. Freed

Sandia National Labs
ATTN: R. Gregory
ATTN: W. Dawes
ATTN: F. Coppage
ATTN: J. Barnum
ATTN: J. Hood
ATTN: M. Knoll

OTHER GOVERNMENT AGENCIES

Department of Commerce
National Bureau of Standards
ATTN: R. Scace
ATTN: W. Bullis
ATTN: S. Chappell
ATTN: J. Mayo-Wells
ATTN: K. Galloway
ATTN: J. Humphreys
ATTN: J. French

NASA
Goddard Space Flight Center
ATTN: J. Adolphsen
ATTN: V. Danchenko

NASA
George C. Marshall Space Flight Ctr
ATTN: M. Nowakowski
ATTN: L. Haniter
ATTN: EG02

NASA
ATTN: J. Murphy

OTHER GOVERNMENT AGENCIES (Continued)

NASA
Lewis Research Center
ATTN: M. Baddour

NASA
Ames Research Center
ATTN: G. Deyoung

NASA
Langley Research Center
ATTN: H. Hendricks

Naval Avionics Center
ATTN: D813, R. Katz

NASA/GSC
ATTN: W. Reed

DEPARTMENT OF DEFENSE CONTRACTORS

BDM Corp
ATTN: D. Wunch
ATTN: D. Alexander
ATTN: R. Pease

Boeing Company
ATTN: R. Caldwell

Burr-Brown Research Corp
ATTN: H. Smith

Charles Stark Draper Lab, Inc
ATTN: C. Lai
ATTN: P. Greiff
ATTN: P. Kelly
ATTN: A. Freeman
ATTN: R. Bedingfield
ATTN: A. Schutz
ATTN: R. Ledger

Ford Aerospace & Communications Corp
ATTN: Technical Info Services

General Dynamics Corp
ATTN: W. Hansen

General Dynamics Corp
ATTN: R. Fields
ATTN: D. Wood

General Electric Company/SD
ATTN: J. Andrews
ATTN: J. Peden
ATTN: R. Casey

General Electric Company
ATTN: D. Cole
ATTN: J. Gibson

General Electric Company—TEMPO
ATTN: M. Espig
ATTN: DASIAC

General Electric Company—TEMPO
ATTN: DASIAC

General Research Corp
ATTN: Technical Info Office

DEPARTMENT OF DEFENSE CONTRACTORS (Continued)

Goodyear Aerospace Corp
ATTN: Security Control Station

Grumman Aerospace Corp
ATTN: 741, D. Manzolillo

GTE Sylvania, Inc
ATTN: L. Blaisdell
ATTN: C. Thornhill
ATTN: L. Pauples

GTE Sylvania, Inc
ATTN: J. Waldron
ATTN: H & V Group
ATTN: H. Ullman
ATTN: P Fredrickson

Harris Corp
ATTN: C. Anderson
ATTN: J. Cornell
ATTN: T. Sanders

Honeywell, Inc
ATTN: C. Cerulli

Honeywell, Inc
ATTN: Technical Library

Hughes Aircraft Co
ATTN: R. McGowan
ATTN: J. Singletary

Hughes Aircraft Co
ATTN: D. Shumake
ATTN: E. Smith
ATTN: A. Narevsky
ATTN: W. Scott

Institute for Defense Analyses
ATTN: Tech Info Services

Intel Corp
ATTN: M. Jordan

International Business Machine Corp
ATTN: J. Ziegler

International Tel & Telegraph Corp
ATTN: Dept 608
ATTN: A. Richardson

Litton Systems, Inc
ATTN: J. Retzler
ATTN: G. Maddox

Lockheed Missiles & Space Co, Inc
ATTN: J. Crowley
ATTN: J. Smith

Lockheed Missiles & Space Co, Inc
ATTN: M. Smith
ATTN: D. Phillips/DPT 62-46, Bldg 151
ATTN: C. Thompson
ATTN: E. Smith
ATTN: E. Hessee
ATTN: P. Bene

AD-A092 959 AIR FORCE WEAPONS LAB KIRTLAND AFB NM F/G 20/6
FIBER OPTIC TRANSMITTER AND RECEIVER RADIATION EVALUATION.(U)
SEP 80 B DEVE, K LOREE

UNCLASSIFIED AFWL-TR-79-168 NL

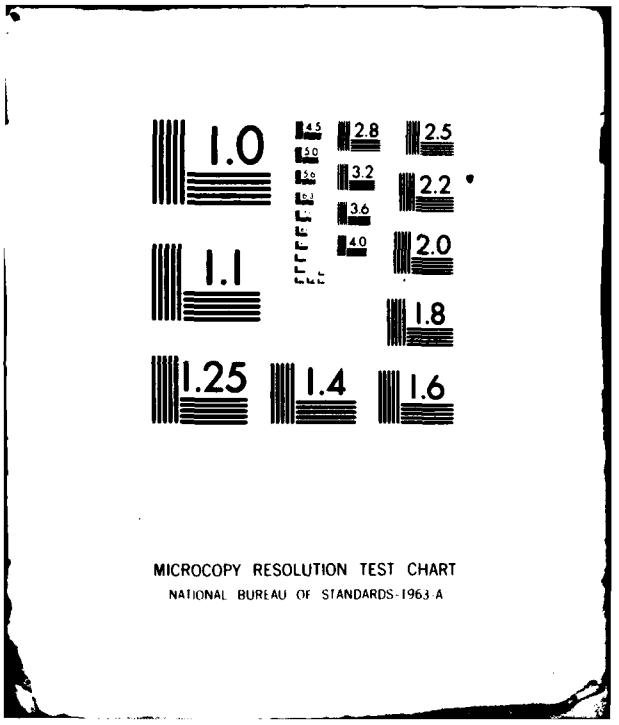
1.0
1.1
1.25
1.4
1.6
1.8
2.0
2.2
2.5
2.8
3.2
3.6
4.0
4.5
5.0
5.6
MICROCOPY RESOLUTION TEST CHART
NATIONAL BUREAU OF STANDARDS-1963-A

DEPARTMENT OF DEFENSE CONTRACTORS (Continued)

M.I.T. Lincoln Lab
ATTN: P. McKenzie

McDonnell Douglas Corp
ATTN: D. Dohm
ATTN: M. Stitch
ATTN: Library

McDonnell Douglas Corp
ATTN: J. Holmgrem
ATTN: D. Fitzgerald

McDonnell Douglas Corp
ATTN: Technical Library

Mission Research Corp
ATTN: C. Longmire

Mission Research Corp
ATTN: R. Pease

Mission Research Corp-San Diego
ATTN: J. Raymond
ATTN: V. Van Lint

Motorola, Inc
ATTN: L. Clark

National Academy of Sciences
ATTN: R. Shane

National Semiconductor Corp
ATTN: R. Wang
ATTN: A. London

University of New Mexico
ATTN: H. Southward

Northrop Corp
ATTN: J. Srour
ATTN: P. Eisenberg
ATTN: T. Jackson
ATTN: J. Anderson

Northrop Corp
ATTN: L. Apodaca
ATTN: P. Gardner

R & D Associates
ATTN: C. MacDonald
ATTN: R. Poll
ATTN: S. Rogers

Rand Corp
ATTN: C. Crain

Raytheon Co
ATTN: J. Ciccio

Raytheon Co
ATTN: H. Flescher
ATTN: A. Van Doren

RCA/GSD/AE
ATTN: G. Brucker
ATTN: V. Mancino

RCA Corp
ATTN: Office N103
ATTN: D. O'Connor

DEPARTMENT OF DEFENSE CONTRACTORS (Continued)

RCA Corp
ATTN: E. Van Keuren
ATTN: J. Saultz

RCA Corp
ATTN: W. Allen

Rockwell International Corp
ATTN: V. Michel
ATTN: G. Messenger
ATTN: J. Brandford
ATTN: V. De Martino
ATTN: V. Strahan

Rockwell International Corp
ATTN: D. Stevens

Rockwell International Corp
ATTN: T. Yates
ATTN: TIC BA08

Rockwell International Corp
ATTN: D. Vincent

Singer Company
ATTN: J. Brinkman

Singer Company
ATTN: R. Spiegel

Sperry Rand Corp
ATTN: P. Maraffino
ATTN: F. Scaravaglione
ATTN: R. Viola
ATTN: C. Craig

Sperry Rand Corp
ATTN: D. Hedger

Texas Instruments, Inc
ATTN: A. Peletier
ATTN: R. Stehlin

Texas Instruments, Inc
ATTN: F. Poblenz

TRW Defense & Space Sys Group
ATTN: M. Sharma

TRW Defense & Space Sys Group
ATTN: F. Fay
ATTN: R. Kitter
ATTN: W. Willis
ATTN: M. Gorman

TRW Systems & Energy
ATTN: B. Gililland
ATTN: G. Spehar

Vought Corp
ATTN: Library

Westinghouse Electric Co.
ATTN: L. McPherson

Westinghouse Electric Corp
ATTN: H. Kalapaca
ATTN: D. Crichi
ATTN: J. Henderson